Methane profiles from GOSAT thermal infrared spectra

Arno de Lange[1] and Jochen Landgraf[1]

[1]SRON Netherlands Institute for Space Research, Utrecht, The Netherlands

Correspondence to: Arno de Lange (A.de.Lange@sron.nl)

Abstract.

1 Introduction

General

We would like to thank both reviewers for the constructive comments that aided us to improve our manuscript. In this document we provide our replies to the reviewer's comments. The original comments made by the reviewer are typeset in italic font. Following every comment we give our reply. We provide a new version of the manuscript but in our replies to the comments we provide line numbers, page numbers and figure numbers referring to the original version of the manuscript, if not stated differently.

Response to Referee #1

Minor Comment 1

P1, L6: Make clear the MACC model profiles are scaled to match the TCCON observations. i.e. "scaled to the TCCON total column". The phrasing on P2, L30-33 is more clear.

Changes: Wording of P1, L6 is now in line with phrasing on P2, L30-33.

Minor Comment 2

P1, L20-21: Some wildfires are also "natural" sources of CH4, so this discussion should be reworded.

Changes: Clear distinction is made between natural and anthropogenic sources (P1, L20-21).

Minor Comment 3

P1, L25-26 and P2, L3: Please provide a few references for these statements – I agree with them, you just need references to support them in the text.

Changes: Two references have been added to support both statements (P1, L25-26 and P2, L3).

Minor Comment 4

P2, L4-9: Also include the Cross-track Infrared Sounder aboard the Suomi-NPP satellite.

Changes: At the end of P2, L9, CRiS aboard Suomi-NPP has been added to the listed satellite instruments.

Minor Comment 5

P2, L35: I don't think you need to note that the correction scheme helps here, as if it didn't you probably wouldn't be publishing it.

Changes: P2, L35-P3, L2 have been re-worded.

As a stand-alone sentence the referee would be right. However, in the article this particular sentence is used as a bridge to the following line. To prevent confusion, the two sentences have been re-worded.

Minor Comment 6

P3, L6-19: I would appreciate more discussion of GOSAT in the main text of the paper, specifically on the spectral resolution of the infrared band and on any known instrument or retrieval issues with the thermal infrared observations.

Changes: We have added the spectral resolutions of the bands (P3, L11). Regarding instrumental issues, there is the concern that a small non-linearity is unaccounted for in the L1b version used in this study, which is also added to the text (P3, L18).

We are not aware of specific GOSAT retrieval issues. There is, however, a general observation of a (positive) bias in methane TIR retrievals that is not fully understood, as already mentioned in the text (P2, L13-22).

Minor Comment 7

P4, L14: What version of the MT_CKD continuum did you use? The reference discusses several different versions.

Changes: Version MT_CKD_2.5 has been added (P4, L14)

Minor Comment 8

P4, L20-22: Can you provide more details on how the actual line-by-line calculation is done?

Changes: The line-by-line calculation follows the RemoTeC implementation and this remark has been added to the text with the proper reference (P4, L19).

Minor Comment 9

P8, L10: This is not true as stated, as you have just shown in Figure 1 that the sensitivity of the methane retrieval varies quite a bit with altitude. I think you are trying to say that, after the averaging kernel of GOSAT is applied to the MACC/TCCON columns, they have similar sensitivity and thu can be compared? If so, that is not currently clear in the text.

Changes: For clarity SWIR is now explicitedly mentioned in P8, L8.

I believe there is a misunderstanding here. Figure 1 refers to TIR averaging kernels, but the statement (P8, L10) refers to SWIR retrievals and Figure 1 is therefore not relevant in this discussion (nor mentioned in the text). For the SWIR retrievals the statement is, to a very high degree, true. To avoid confusion SWIR is now explicitedly mentioned in the text.

Minor Comment 10

P9, L16-19: I'm not convinced that this cloud-clearing algorithm is sufficient for the type of validation study you are doing here. Did you make any independent checks to confirm that the cloud-filtered profiles were likely cloud free, say using independent observations from other bands for the daytime cases? How large of a cloud AOD can your procedure miss?

No changes.

In this study we actually used the method proposed by the referee to check the cloud filter against the independent observations from the SWIR bands (P20, L3-11) and the quality of the filter is sumarised in Table 1 on P20.

The suggestion by the referee to identify the detection limit in terms of cloud optical depth, sounds reasonable and is actually a quantity provided by the SWIR filter. However, there are two reasons for not including this in the current study: First, the cloud optical depth from the SWIR filter is not a validated product, but merely a filter quantity, and secondly, the cloud optical depth alone is of limited use only since the vertical sensitivity of the TIR retrievals. For instance, a thick low cloud may be missed by the TIR filter, without impacting the retrievals because of the loss of sensitivity towards the surface.

We have shown that the performance of the TIR and SWIR filters are almost identical in terms of biases (Table 1, P20), but the spread is larger in case for the TIR cloud filter (Table 1, P20). Therefore we believe that this (admittedly crude) cloud filter does not introduce additional biases (which is the focus of the current study) and we propose to leave the text as is.

Minor Comment 11

P9, L21: Is the chi-squared check considered part of the cloud filter?

No changes.

Yes, the chi-squared check is indeed considered part of the cloud filter, which is in correspondence with the cloud filter from the SWIR bands. This test identifies the failure of the forward model to capture all spectral features of the observation. The forward model does not account for clouds, and a large chi-squared may therefore indicate the occurence of clouds in the observation.

Typos and Style Suggestions 1

P1, L18 and L20: I'd say "the year 1750" in both places, as the first time I read this I thought you were saying this was the pre-industrial concentration of CH4 in ppbv.

Changes: As per suggestion (P1, L18 and L20).

Typos and Style Suggestions 2

P2, L24: Check the format of these references.

Changes: The references are now correct (P2, L24).

Typos and Style Suggestions 3

P7, L18: typo in "A priori"

Changes: As per suggestion (P7, L18).

Typos and Style Suggestions 4

P9, L12: I'm not sure what "we pertain to" means here, I think you mean something like "we focus on"

Changes: As per suggestion (P9, L12).

Typos and Style Suggestions 5

P11, L6: This is a bar chart, not a histogram.

Changes: As per suggestion (P11, L6).

Response to V. Payne (Referee #2)

Comment 1

In general: How good are the MACC CH4 profiles? Can the authors provide any references to model validation? Are the profile comparisons sensitive to uncertainties in the model representation of the stratosphere?

Changes: A second verification study has been added to the text (P10, L1)

The quality of the MACC fields are being discussed in lines P9,L29-P10,L3. In these lines we refer to a study verifying that the model delivers methane fields within 1% uncertainty, albeit with different input data as used in the current setup (NOAA-ESRL as opposed to GOSAT-SWIR). For completeness, we have now added a second reference in which the MACC fields (based on SCIAMACHY data) are verified to be again within 1% with independent observations. We have estimated the uncertainty in the current setup to be 2%, which seems therefore to be on the safe side.

Comment 2

Abstract, lines 14-15: "This filter. . ..is consistent with the cloud filter based on the GOSAT-SWIR measurements, despite the fact that the TIR-filter is less stringent". I was not clear on what this means. When you say the filter is consistent, do you mean that the bias in the retrieved profile does not change according too which filter is used? Consider changing the wording to say that the bias (rather than the filter) is consistent?

Changes: Abstract L14-15 have been adapted to clearly state that a) no additional biases are introduced by the TIR-filter (wrt. SWIR) and b) the acceptance rate of observations is higher for the TIR-filter but the uncertainty as well (wrt. SWIR)

Comment 3

Page 2, lines 1-12: Please also list the Cross-track Infrared Sounder (CrIS). There is a CrIS flying on the Suomi-NPP satellite, launched in 2011, and there will be follow-on instruments on the JPSS satellite series. I am not aware of a publication on CrIS CH4 retrievals to date, but there are definitely people working on those.

Changes: At the end of P2, L9, CRiS aboard Suomi-NPP has been added to the listed satellite instruments.

Comment 4

Page 2, lines 23-29: This discussion of previous work is a little hard to follow and would benefit from some re-wording for clarification of various points. Papers from Saitoh (2012) and Holl (2016) cannot both present "first results". It would be helpful to clarify that the Saitoh (2012), Holl (2016) and Zhou (2016) papers all discuss GOSAT TIR results from the same algorithm, and that algorithm is different from the one that you are using here.

Changes: "First" has been omitted (P2, L24). The statements that these papers stem from the same algorithm and we use a different one, are included (P2, L30).

Comment 5

(Degree of signal should be degrees of freedom for signal?) When you say that the degrees of freedom for signal are significantly lower than 1, are you referring to the degrees of freedom for signal in that other algorithm? This was not totally clear from the text.

Changes: It should indeed be "degrees of freedom for signal" and has been adapted (P2, L26). Two other occurences in the text have been adapted as well (P2, L30 and P6, L3). We were indeed referring to the other algorithms and this has now been made explicit (P2, L26).

Comment 6

Zhou et al. (2016) compare results from AIRS (not IASI) and GOSAT. The statement about "A prevalent bias. . .between both satellite retrievals" is confusing. Since the Zhou et al. paper does not appear to include any independent validation measurements and deals only with a comparison between two satellite retrievals, I assume that you are referring purely to the difference between the retrievals, in which case, you should state clearly which one is biased high relative to the other. As an aside, a point that is not discussed in the Zhou et al. paper, but which has been referred to in AIRS papers and presentations (for example, in Xiong et al. [2008]) is that in those AIRS CH4 retrievals, absorption coefficients are tuned within the radiative transfer algorithm in order to produce better agreement with validation data (a different form of correction). Xiong, X., C.

Barnet, E. Maddy, C. Sweeney, X. Liu, L. Zhou, and M. Goldberg (2008), Characterization and validation of methane products from the Atmospheric Infrared Sounder (AIRS), J. Geophys. Res., 113, G00A01, doi:10.1029/2007JG000500.

Changes: The confusion between IASI and AIRS has been cleared (P2, L28). It is now explicitedly stated that AIRS is biased high wrt. GOAST (P2, L27-29). The bias correction approach in the AIRS retrievals has been added to the discussion (P2, L14).

Comment 7

Page 2, lines 34-36: I think it would be good to refer here to the use of a similar correction approach using empirical orthogonal functions within the OCO-2 Level 2 algorithm. To my knowledge, the OCO-2 approach is not discussed in any journal papers to date, but you can find discussion of the use of empirical orthogonal functions in the OCO-2 Algorithm Theoretical Baseline Document (ATBD), available at: https://docserver.gesdisc.eosdis.nasa.gov/public/project/OCO/OCO2_L2_ATBD.V6.pdf

Changes: We agree that the approach by the OCO-2 team is very similar and we have added this to the text (P3, L2), including the reference.

Comment 8

Page 3, line 27: It is not clear to me what is meant by "an effective H2O column to calculate the water continuum independently from the water vapor absorption lines." Can you please expand on this point?

Changes: P3, L27 has been re-worded.

It turned out that a single water retrieval parameter was not sufficient to capture the spectral features of both the water vapour absorption lines and the continuum contribution. Therefore, two parameters are in the state vector incorporated to account for both contributions respectively. The text has been expanded to make this point clear.

Comment 9

Page 6, Fig 1: Please label the altitude axis on the right hand side of the figure.

Changes: Fig 1 (P6) has been changed. For similar reasons Figs 2 (P8), 5 (P12), and 6 (P13) have been changed as well.

Comment 10

Page 7, line 1: Suggest removing the word "reduced".

Changes: As per suggestion (P7, L1).

Comment 11

Page 7, lines 18-19: "the fact that the null space contribution of the integrated methane column is typically in the order of 30 %". Did you show this somewhere? Please elaborate.

Changes: An explicit explanation has been added to the text (P7, L18) with a reference to Figure 2 (P8).

Comment 12

Page 9, line 7: Suggest replacing "cloud clearing" with "cloud screening", since the term cloud clearing has a particular meaning to some members in the TIR sounding community (Susskind et al., 2003). Susskind et al., IEEE TRANSACTIONS ON GEOSCIENCE AND REMOTE SENSING, VOL. 41, NO. 2, FEBRUARY 2003

Changes: As per suggestion (P9, L17). An other occurence has been updated as well (P20, L5).

Comment 13

Page 10, line 9: "Indicatory" is not a word that would be commonly used. Suggest saying instead that the difference is representative.

Changes: As per suggestion (P10, L9).

Comment 14

Page 11, Figure 4: Why choose this order for the TCCON stations? Consider arranging them by latitude.

No changes.

It is the processing order and we did not put much thought into the arrangment of the figures. Rearranging them would only make sense when the order is rearranged in all figures, charts and tables. However, this needs to be done manually and is therefore error prone. We would like to request if keeping the current, admittedly peculiar, order is acceptable, as it will not lead to different conclusions or insights.

Grammar/typographical errors 1

Page 3, line 14: Suggest splitting the points about the 10 km footprint and the sparse spatial sampling into two separate sentences for clarity.

Changes: As per suggestion (P3, L12-14).

Grammar/typographical errors 2

Page 3, line 15: Coarse should be course.

Changes: As per suggestion (P3, L15).

Grammar/typographical errors 3

Page 3, line 16: Should this be v160160?

No changes.

During the reprocessing of the data under v160160, a small update was incorporated leading to v161160. It was decided to only process the remaining data under v161160 and keep the already processed data under v160160. Therefore the version is generally indicated as v16x160.

Grammar/typographical errors 4

Page 2, line 15: Tropospherical should be tropospheric.

Changes: As per suggestion (P2, L15).

2 Conclusions

References

Methane profiles from GOSAT thermal infrared spectra

Arno de Lange[1] and Jochen Landgraf[1]

[1]SRON Netherlands Institute for Space Research, Utrecht, The Netherlands

Correspondence to: Arno de Lange (A.de.Lange@sron.nl)

Abstract. This paper discusses the retrieval of atmospheric methane profiles from the thermal infrared band of the Japanese Greenhouse Gases Observing Satellite (GOSAT) between 1210 and 1310 cm^{-1}, using the RemoTeC analysis software. Approximately one degree of information on the vertical methane distribution is inferred from the measurements with the main sensitivity at about 9 km altitude but little sensitivity to methane in the lower troposphere. For verification, we compare the GOSAT methane abundance at measurement sites of the Total Carbon Column Observing Network (TCCON) to methane profiles provided by the Monitoring Atmospheric Composition and Climate (MACC) model fields scaled to the total column observations at the sites. For verification, we compare the GOSAT-TIR methane profile retrieval results with profiles from model fields provided by the Monitoring Atmospheric Composition and Climate (MACC) project, scaled to the total column measurements of the Total Carbon Column Observing Network (TCCON) at ground-based measurement sites. Without any radiometric corrections of GOSAT observations, differences between both data sets can be as large as 10%. To mitigate these differences, we developed a correction scheme using a principal component analysis of spectral fit residuals and airborne observations of methane during the HIAPER Pole-to-Pole Observations (HIPPO) campaign II and III. When the correction scheme is applied, the bias in the methane profile can be reduced to less than 2% over the whole altitude range with respect to MACC model methane fields. Furthermore, we show that, with this correction, the retrievals result in smooth methane fields over land and ocean crossings and no differences are to be discerned between daytime and nighttime measurements. Finally, a cloud filter is developed for the nighttime and ocean measurements. This filter is rooted in the GOSAT-TIR measurements and is consistent with the cloud filter based on the GOSAT-SWIR measurements, despite the fact that the TIR-filter is less stringent. This filter is rooted in the GOSAT-TIR measurements and its performance, in terms of biases, is consistent with the cloud filter based on the GOSAT-SWIR measurements. The TIR filter shows a higher acceptance rate of observations than the SWIR filter, at the cost of a higher uncertainty in the retrieved methane profiles.

1 Introduction

Methane (CH_4) is, after carbon dioxide (CO_2), the strongest anthropogenic greenhouse gas with an estimated total radiative forcing of 0.97 $\mathrm{W/m}^2$ for 2011 with respect to the pre-industrial levels of the year 1750 (Myhre et al., 2013). The forcing per molecule is ≈100 times stronger than that of carbon dioxide, but the abundance is ≈200 times lower. The current relative increase with respect to pre-industrial background levels of the year 1750 is 150% for methane, as opposed to 40% for carbon dioxide. Natural methane sources are anaerobic environments where micro-organisms convert organic material into methane.

Examples are wetlands including swamps, boreal marshes, and tundras, but also lakes and oceans are natural methane sources. In line with these natural processes are the cultivation of rice paddies and cattle, both anthropogenic sources. Other anthropogenic sources include the burning of organic material (biomass burning and waste burning), and gas losses in the fossil fuel industry (Myhre et al., 2013). Other sources include the burning of organic material, such as biomass burning (both natural and anthropogenic) and waste burning (anthropogenic), and gas losses in the fossil fuel industry (anthropogenic) (Myhre et al., 2013). For climate monitoring and prediction, it is essential to measure CH_4 on a global scale and information on its vertical distribution may help to disentangle signals due to methane surface emissions and long-range transport Jacob et al. (2016); Bousserez et al. (2015).

Satellite nadir measurements of CH_4 in the thermal infrared (TIR) represent an important element of a climate observing system because of the pronounced methane sensitivity of the measurements in the upper troposphere. Therefore, these measurements can aid in the decoupling of methane emissions and transport in inverse-modeling studies REFERENCE NEEDED: ANY IDEA??. Currently five nadir-viewing instruments in the thermal infrared are operational on satellite platforms; Atmospheric InfraRed Sounder (AIRS), aboard Aqua, launched in 2002 (Xiong et al., 2008; Zou et al., 2016); Tropospheric Emission Spectrometer (TES), aboard AURA, launched in 2004 (Wecht et al., 2012; Worden et al., 2012, 2015); Infrared Atmospheric Sounding Interferometer (IASI), aboard Metop-A and Metop-B, launched in respectively 2006 and 2012 (Razavi et al., 2009; Crevoisier et al., 2013; Cressot et al., 2014; Siddans et al., 2016); Thermal and Near infrared Sensor for Carbon Observation - Fourier Transform Spectrometer (TANSO-FTS) aboard GOSAT, launched in 2009; Cross-track Infrared Sounder (CrIS), aboard Suomi-NPP, launched in 2011 (**?**) –> Volume 118, 2013 Pages 12,734–12,748 to be included in bib-file. Furthermore, GOSAT-2, the successor of the GOSAT satellite, will also be equipped with two thermal infrared bands (together covering the same wavelength range as the one TIR band in GOSAT) and a new generation of IASI spectrometers (IASI-NG) will fly on three successive Metop-SG A satellites of the EUMETSAT Polar System of Second Generation (EPS-SG) in the 2021-2040 time frame.

In many studies on methane retrievals from thermal infrared observations of the above mentioned satellites, a bias in the methane product is observed. To address this bias, different approaches have been adopted. Xiong et al. (2008) improves the AIRS CH_4 validation results by tuning absorption coefficients within the radiative transfer algorithm. Worden et al. (2012) observes a discrepancy between upper and lower tropospheric**al**tropospheric methane of ≈ 4 % in case of TES observations and mentions uncertainties in temperature, calibration inaccuracies and spectroscopy errors as the main causes. A CH_4/N_2O proxy retrieval reduces this bias to $\approx 2.8\%$ but does not fully remove it. Siddans et al. (2016) also observes a bias of $\approx$4% and scales the methane mixing ratios retrieved from IASI measurements. Furthermore, two additional scaling parameters are fitted for the mean residual of respectively nadir observations and at the outer edge of the swath, to account for variations in interfering water vapor and scan mirror errors. The resulting methane product is within 2% of HIPPO over the full altitude range. Also Crevoisier et al. (2013) applies a radiometric correction based on mean residuals in case of IASI measurements. Finally, von Clarmann et al. (2009) mentions that 8 micro-windows are carefully selected for the MIPAS limb retrievals to reduce the known high bias of CH_4.

The current study focuses on the retrieval of methane profiles from GOSAT observation in the thermal infrared band 1210–1310 cm^{-1}. Previous work by Saitoh et al. (2012); Holl et al. (2016) presented first results of GOSAT-TIR retrievals of methane, where the measurements are radiometrically corrected using the approach of Saitoh et al. (2009). Previous work by Saitoh et al. (2012); Holl et al. (2016) presented results of GOSAT-TIR retrievals of methane, where the measurements are radiometrically corrected using the approach of Saitoh et al. (2009). Spectral residuals in GOSAT are assessed with measurements of buoys and are subsequently accounted for in the retrievals. HereIn these studies, the degree of freedom for signal for the retrieval is significantly lower than 1. Moreover, Zou et al. (2016) compared the retrieval of methane profiles from GOSAT and IASI thermal infrared measurements and observed a prevalent bias at 9 km altitude of about 3% between both satellite retrievals. Moreover, Zou et al. (2016) compared the retrieval of methane profiles from GOSAT and AIRS thermal infrared measurements and observed a prevalent bias at 9 km altitude of about +3% between both satellite retrievals (AIRS minus GOSAT).

In the GOSAT-TIR studies mentioned above, the retrieval results stem from the same algorithm. In this study, we use a different algorithm and we apply the RemoTeC retrieval tool to analyse the GOSAT-TIR measurements with a degree of freedom for signal (DOFS) ≈ 1 and verify the retrieval results with profiles of the Monitoring of Atmospheric Composition and Climate (MACC) project scaled to the total column measurements of the Total Carbon Column Network (TCCON) at ground-based measurements sites. To mitigate the observed significant biases, we developed a sophisticated correction scheme based on a principal component analysis of spectral residuals using HIPPO (HIAPER Pole-to-Pole Observations) data as an estimate for the atmospheric state. This correction scheme improves significantly our validation. Moreover, we achieve the consistency of daytime and nighttime measurements as well as continuity of methane for land–sea crossings where the measurement sensitivity to methane in the lower and middle atmosphere changes substantially. Not only does this correction scheme significantly improve our validation, we also achieve the consistency of daytime and nighttime measurements as well as continuity of methane for land–sea crossings where the measurement sensitivity to methane in the lower and middle atmosphere changes substantially. It is noted that a similar correction approach, using empirical orthogonal functions, is being used within the OCO-2 Level 2 algorithm OCO-2.

The article is structured as follows: in Section 2 the GOSAT-TIR measurements are introduced, Section 3 introduces the Tikhonov regularisation scheme to invert the measurements. Finally, Section 4 presents the bias correction scheme and its effect on the retrievals is demonstrated.

2 GOSAT

The Japanese satellite GOSAT (Greenhouse gases Observing SATellite) was launched in 2009 and is the world's first satellite fully dedicated to the monitoring of the two most important greenhouse gases — carbon dioxide and methane. Its main instrument is the TANSO-FTS Fourier Transform spectrometer covering four wavelength bands; the oxygen A-band ($\approx$ 13000 cm^{-1}), two bands in the shortwave infrared regime ($\approx$ 5000 $\mathrm{cm}^{-1}$and $\approx$ 6200 cm^{-1}), and a band in the thermal infrared wavelength range ($\approx$ 600–1600 cm^{-1}). The spectral resolution of the oxygen A-band is ≈ 0.5 cm^{-1}, whereas the other three bands show a resolution of ≈ 0.27 cm^{-1}. This study focuses only on the retrieval of methane for the thermal infrared (TIR)

band, employing the spectral window 1210–1310 cm^{-1}. TANSO-FTS has an instantaneous field of view of ≈ 10 km allowing for high spatial resolution measurements with at the same time a sparse spatial sampling. Here, the distance between two consecutive measurements is up to several 100 km. TANSO-FTS has an instantaneous field of view of ≈ 10 km allowing for high spatial resolution measurements. The spatial sampling, on the other hand, is sparse with a distance between two consecutive measurements of up to several 100 km.

Over the coarse course of the mission, JAXA (Japan Aerospace Exploration Agency) has released several level 1B data versions, and in this study v16x160 of L1B data has been used. For the TIR band, this version contains important updates with respect to previous versions (such as updated radiometric correction parameters, polarization effects, and reference blackbody emissivity) and is virtually identical to the most recent version v201202, however there is a concern that a small non-linearity is still unaccounted for. For further details on the instrument, its calibration, and performance, we refer to Kuze et al. (2009, 2014, 2016).

3 Retrieval

To infer methane profiles from GOSAT-TIR measurements, a forward model $\boldsymbol{F}$ is needed, that simulates the radiance measurement $\boldsymbol{r}$ as function of the atmospheric state vector,

$$\boldsymbol{r} = \boldsymbol{F}(\boldsymbol{x}, \boldsymbol{b}) + \boldsymbol{e_y}, \tag{1}$$

where $\boldsymbol{e_y}$ comprises forward model error and instrument error including the measurement noise. The state vector $\boldsymbol{x}$ contains all parameters to be retrieved from the measurement and consists of the methane profile (defined over 12 layers at equidistant pressure levels), the skin temperature, a spectral shift, and four scaling parameters for the total columns of H_2O, HDO, N_2O, and an effective total H_2O column to calculate the water-continuum independently from the water vapour absorption lines. and a separate total H_2O column to calculate the water-continuum. The inclusion of this separate water column in the state vector is necessary as the forward model can not capture all water-related spectral features of both the water vapour absorption lines and the water continuum contribution, with a single parameter. The forward model parameter $\boldsymbol{b}$ symbolises all model parameters that require prior knowledge, such as instrument parameters, atmospheric pressure and temperature profiles.

3.1 Forward model

To simulate line-by-line radiance spectra at the top of the model atmosphere, we account for the Planck radiation of the Earth surface and its atmosphere as radiation source and ignore the solar contribution to the spectrum analogous to e.g. Wassmann et al. (2011). For a non-scattering atmosphere, the down-welling radiation is reflected by the Earth surface assuming isotropic Lambertian reflection. The down-welling is calculated by the means of a 4-point Gaussian quadrature. The wavelength-dependent emission by the Earth's surface is a function of surface temperature and the surface emissivity. Here, the surface reflection of down-welling atmospheric radiation is governed by the emissivity, following Kirchhoff's law. We determine the initial surface emissivity over land with the High Spectral Resolution Algorithm developed by Borbas (Borbas et al.,

2007; Borbas and Ruston, 2010) using the University of Wisconsin Baseline Fit (UW-BF) Emissivity Database (Seemann et al., 2008) as input. For water surfaces, we use the IRSSE model by van Delst and Wu (2000) to calculate the surface emissivity in RemoTeC. This model is an update of Wu and Smith (1997) and the calculated emissivity is a function of sea-roughness as determined by the wind speed, viewing angle, and wavelength of the radiation. Furthermore, we consider atmospheric absorption by H_2O, CH_4, N_2O, and CO_2 from the HITRAN 2008 database (Rothman et al., 2009) and describe atmospheric continuum absorption using the MT_CKD_2.4 model by Mlawer et al. (2012) to account for broad-band contributions from water, carbon dioxide, oxygen, nitrogen, and ozone. Here the continuum contribution by water is calculated separately, including the foreign and self continuum. The surface temperature and wind speed as well as the water vapour and temperature profile of the atmosphere, needed to initialise the retrieval, are taken from European Centre for Medium-Range Weather Forecast (ECMWF) ERA interim data set (Dee et al., 2011). The CH_4 and N_2O profiles are adapted from MACC-II (Bergamaschi and Alexe, 2014), and CO_2 from CarbonTracker CT2013 (Peters et al., 2007; CarbonTracker website). The line-by-line calculation follow the RemoTeC implementation as described in (Butz et al., 2011; Schepers et al., 2012).

Finally the line-by-line spectra are degraded to the spectral resolution of the sensor using TANSO-FTS spectral response. Numerically, the forward model is implemented in the RemoTeC retrieval tool (Butz et al., 2011; Schepers et al., 2012) to benefit from the overall processing properties of this framework.

3.2 Inversion

The goal of a retrieval is to determine the atmospheric state vector $\boldsymbol{x}$ in Eq. (1) by inverting the forward model $\boldsymbol{F}$. The RemoTeC inversion module is described in detail by Butz et al. (2011) and in this section we summarise the inversion aspects that are relevant for this study.

Since the forward model $\boldsymbol{F}$ is generally not linear in the state vector $\boldsymbol{x}$, Eq. (1) is inverted with a Gauss–Newton iteration scheme. This means that $\boldsymbol{F}$ is linearised in each iteration step by a Taylor expansion around the solution of the previous step, starting with a first guess state vector $\boldsymbol{x}_0$. Equation (1) can be rewritten as

$$\boldsymbol{y} = \mathbf{K}\boldsymbol{x} + \boldsymbol{e_y}, \tag{2}$$

where $\boldsymbol{y} = \boldsymbol{r} - \boldsymbol{F}(\boldsymbol{x}_{i-1}) + \mathbf{K}\boldsymbol{x}_{i-1}$ is the so-called measurement vector with $\boldsymbol{x}_{i-1}$ the state vector of the previous iteration step and $\mathbf{K}$ is the Jacobian matrix.

To infer a vertical methane profile from GOSAT-TIR measurements represents an ill-posed problem requiring regularisation. Several techniques have been developed to solve such problems and in this study we employ 0-th order Tikhonov regularisation (Tikhonov, 1963; Phillips, 1962; Twomey, 1963):

$$\boldsymbol{x}_\gamma = \min_{\boldsymbol{x}} \left(\|(\mathbf{K}\boldsymbol{x} - \boldsymbol{y})\|^2 + \gamma^2 \|\boldsymbol{x}\|^2 \right), \tag{3}$$

where $\boldsymbol{x}_\gamma$ is the solution vector of the minimisation problem, $\|(\mathbf{K}\boldsymbol{x} - \boldsymbol{y})\|^2$ is the least squares norm and $\|\boldsymbol{x}\|^2$ is the side constraint. γ is the regularisation parameter and has to be carefully chosen to balance the two contributions of the cost function. In this study, we employ the L-curve paradigm to find the appropriate value for the regularisation parameter (Hansen, 1992),

which is discussed extensively in the literature (O.P. Hasekamp, 2001; Steck, 2002; Butz et al., 2011). The solution of Eq. (3) is

$$\boldsymbol{x}_\gamma = \mathbf{D}\boldsymbol{y}, \tag{4}$$

where

$$\mathbf{D} = \left(\mathbf{K}^{\mathrm{T}}\mathbf{K} + \gamma^2\mathbf{I}\right)^{-1}\mathbf{K}^{\mathrm{T}}\mathbf{S}_{\boldsymbol{y}}^{-\frac{1}{2}}, \tag{5}$$

is the pseudo-inverse of $\mathbf{K}$ or the contribution matrix, $\mathbf{S}_{\boldsymbol{y}}$ the measurement noise covariance matrix and $\mathbf{I}$ represents the unity matrix. Moreover, the retrieval noise covariance matrix is given by

$$\mathbf{S}_{\boldsymbol{x}} = \mathbf{D}\mathbf{S}_{\boldsymbol{y}}\mathbf{D}^{\mathrm{T}}, \tag{6}$$

where $\mathbf{S}_{\boldsymbol{y}}$ is measurement noise covariance.

The retrieved vector $\boldsymbol{x}_\gamma$ is a weighted average of the true atmospheric state vector $\boldsymbol{x}_{\mathrm{true}}$

$$\boldsymbol{x}_\gamma = \mathbf{A}\boldsymbol{x}_{\mathrm{true}} + \boldsymbol{e}_{\boldsymbol{x}}, \tag{7}$$

due to the required regularisation. Here $\mathbf{A} = \mathbf{D}\mathbf{K}$ is the averaging kernel and $\boldsymbol{e}_{\boldsymbol{x}} = \mathbf{D}\boldsymbol{e}_{\boldsymbol{y}}$ is the error in the state vector caused by measurement errors. Effectively, the averaging kernel degrades the true profile to the vertical resolution of the retrieval and also defines the null-space contribution of the true state vector $\boldsymbol{x}_{\mathrm{true}}$, namely

$$\boldsymbol{x}_{\mathrm{null}} = (\mathbf{I} - \mathbf{A})\,\boldsymbol{x}_{\mathrm{true}}, \tag{8}$$

comprising the contribution of the state vector, that cannot be inferred from the measurement.

Figure 1 shows a typical averaging kernel for GOSAT-TIR retrievals. It indicates a peak around $9\ \mathrm{km}$, and the retrieval sensitivity drops quickly for altitudes close to surface. This loss in sensitivity to methane concentrations at low altitudes can be understood as follows. Line features only show up in the spectrum if the local photon field is not at equilibrium with the atmospheric radiance corresponding to the Planck curve governed by the ambient temperature. In general, the skin temperature of the Earth is similar to the temperature of the lowest layers of the atmosphere, and the radiance emitted by the Earth's surface is in accordance with the radiances by those atmospheric levels. So, molecular line features are only weakly imprinted on the recorded spectrum, and hence, the sensitivity is very limited.

The degree of freedom for signal (DOFS) is defined by

$$\mathrm{DOFS} = \mathrm{Tr}\,\mathbf{A}, \tag{9}$$

and can be interpreted as the amount of independent pieces of information that can be retrieved from the measurement. In the case of GOSAT-TIR retrievals the DOFS is ≈ 1.0 for scenes with a limited temperature contrast (nighttime measurements or daytime measurements over the ocean) and ≈ 1.1 for daytime measurements over land with on average a slightly higher temperature contrast.

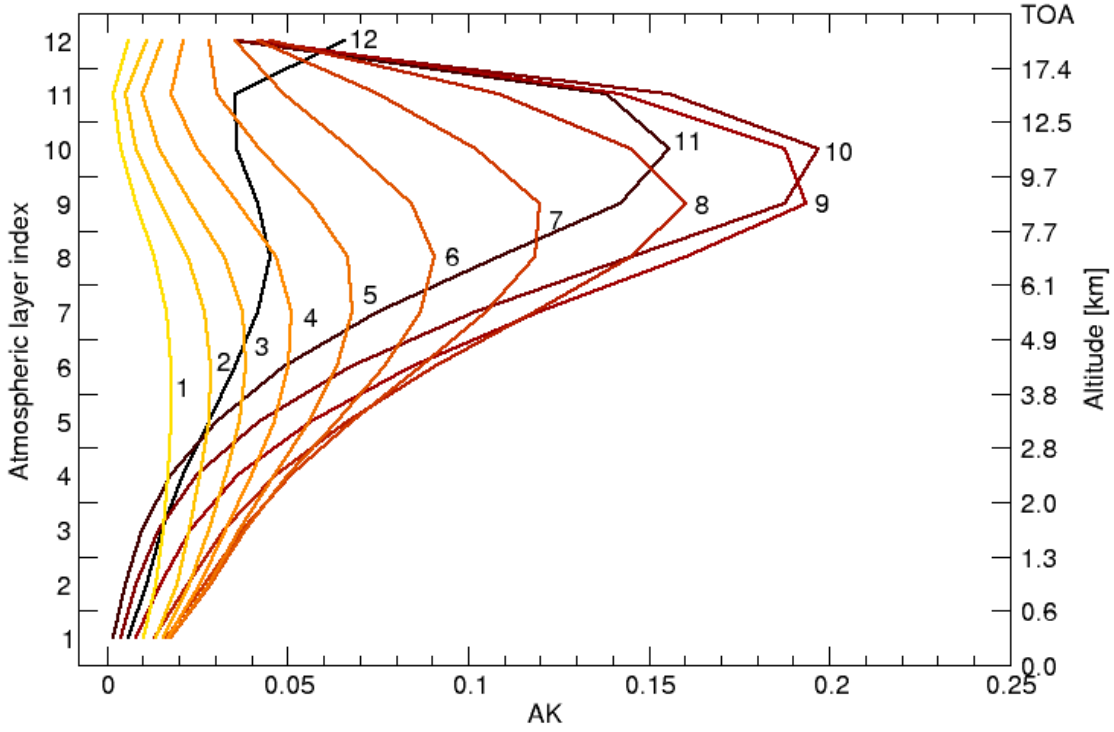

Figure 1. A typical averaging kernels for GOSAT-TIR daytime measurements over land. The colour coding is such that dark colours correspond to the averaging kernels at high altitudes and the bright colours to low altitudes. The numbers next to the curves refer to the corresponding atmospheric layer index as is indicated on the left side of the graph.

When one considers the retrieved profile $\boldsymbol{x}_\gamma$ in Eq. (3) as the methane data product, one has to account for the reduced retrieval sensitivity given by the averaging kernel. Alternatively, one may consider the vertical profile after adding an estimate of the null-space contribution to $\boldsymbol{x}_\gamma$, namely

$$\boldsymbol{x}_{\mathrm{CH_4}} = \boldsymbol{x}_\gamma + (\mathbf{I} - \mathbf{A})\,\boldsymbol{x}_{\mathrm{apr}}, \tag{10}$$

with an a priori estimate of the true profile $\boldsymbol{x}_{\mathrm{apr}}$ coming from e.g. an independent measurement or a chemical transport model forecast. For the purpose of our study, it is also valuable to calculate the total methane column $c_{\mathrm{CH_4}}$ from Eq. (10), namely

$$c_{\mathrm{CH_4}} = \boldsymbol{C}\boldsymbol{x}_{\mathrm{CH_4}}, \tag{11}$$

where $\boldsymbol{C}$ is the column operator, effectively summing all partial columns in $\boldsymbol{x}_{\mathrm{CH_4}}$. This implies that $\boldsymbol{x}_{\mathrm{CH_4}}$ is given in column units, e.g. cm^{-2}. To indicate the actual retrieval sensitivity the so-called column averaging kernel is a useful quantity, defined by the averaging kernel $\mathbf{A}$ and column operator $\boldsymbol{C}$ (Borsdorff et al., 2014)

$$\boldsymbol{A}_{\mathrm{col}} = \boldsymbol{C}\mathbf{A}, \tag{12}$$

as well as the corresponding retrieval error variance

$$\mathrm{s}_{\mathrm{CH_4}} = \boldsymbol{C}\mathbf{S}_{\boldsymbol{x}}\boldsymbol{C}^{\mathrm{T}}. \tag{13}$$

A typical column averaging kernel for land and ocean scenes at daytime and nighttime is depicted in Fig. 2. It shows a clear drop-off in sensitivity towards the lower layers of the atmosphere and also the enhanced sensitivity to the lower layers for daytime measurements over land scenes can be discerned. This enhancement is because of the temperature contrast, which is larger for daytime than for the nighttime measurements and larger for measurements over land than over the ocean.

A priori knowledge on methane has a significant impact on the profile $\boldsymbol{x}_{\mathrm{CH_4}}$, which is indicated by the fact that the null-space contribution of the integrated methane column is typically in the order of 30%. A priori knowledge on methane has a significant impact on the profile $\boldsymbol{x}_{\mathrm{CH_4}}$. This is even the case for the total column as can be determined by applying the column operator $\boldsymbol{C}$ to Eq. 10. The relative contribution of the null-space term $\boldsymbol{C}\left(\mathbf{I}-\mathbf{A}\right)\boldsymbol{x}_{\mathrm{apr}}$ is typically in the order of 30%. This can be estimated from Fig. 2, under the assumption that methane shows a constant profile as function of altitude, by integrating the column averaging kernel over altitude and compare this value to the case of an ideal column averaging kernel of 1 over all altitudes (indicated by a dashed line in the figure). Therefore, the reference profile must be of sufficient quality not to govern the uncertainty in $\boldsymbol{x}_{\mathrm{CH_4}}$.

3.3 Validation approach

Ideally, the validation of the retrieved GOSAT methane profile relies on independent validation measurements of the vertical methane distributions. A promising data source of validation is given by AirCore balloon soundings reaching a height up to 30 km (Karion et al., 2010). However, the development of an extended observation framework is still on-going and to this day the number of usable soundings is very limited causing poor statistics for the validation. Therefore, we decided not to consider these observations in our study. Another validation possibility is to use airborne measurements within the HIPPO (HIaper Pole to Pole Observations) project conducted in the years 2009–2011. Here methane profiles are measured up to ≈ 13 km. In our study, however, these measurements are used to radiometrically correct the GOSAT measurements, as will be shown in Section 4, and can therefore not be used for validation purposes. Finally, during ascent and decent of commercial airlines the methane distribution is measured in-situ close to airports up to typical flight heights of 10 km. Two examples of such measurement frameworks are CONTRAIL (Comprehensive Observation Network for Trace gases by Airliner) (Machida et al., 2008; Inoue et al., 2014) and CARIBIC (Civil Aircraft for the Regular Investigation of the atmosphere Based on an Instrument Container) (Brenninkmeijer et al., 2007). Obviously, these measurements are limited in altitude to typically 10 km and therefore lack an important part of the profile to which the GOSAT-TIR measurement is sensitive to. All in all, high-quality measurements of methane profiles are sparse and due to the required co-location between GOSAT measurements and

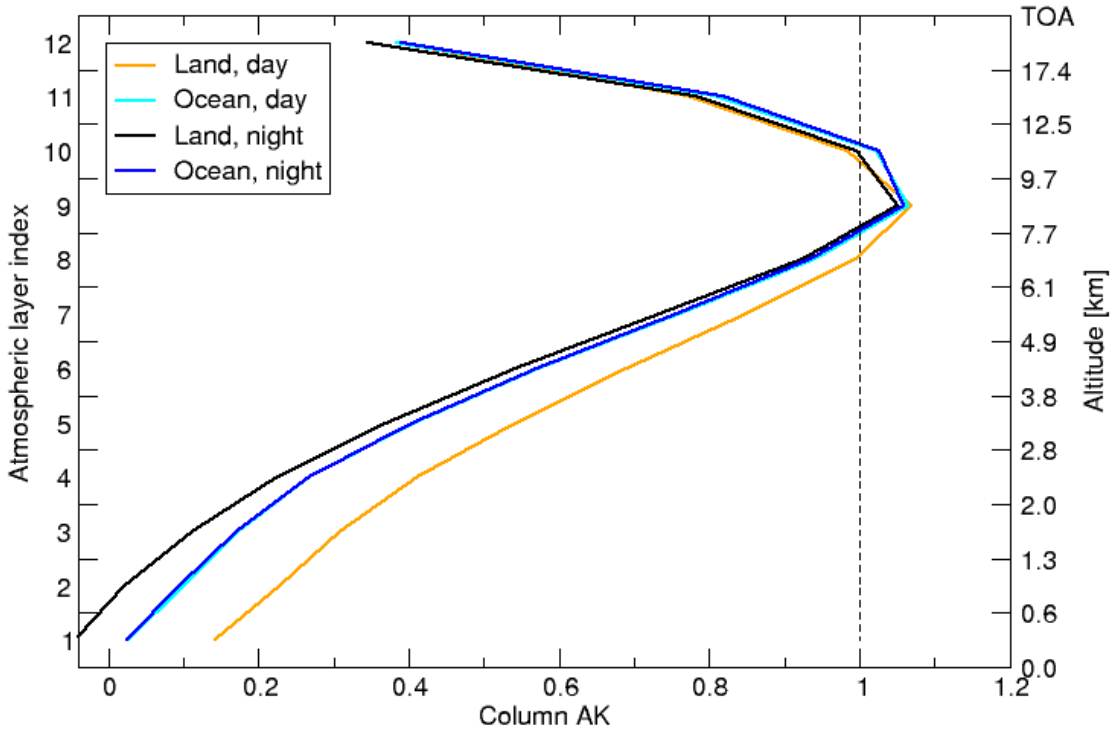

Figure 2. The average of all column averaging kernels in this study for different scenes and measurement times. Daytime and nighttime measurements over land are depicted in respectively orange and black curves and over the ocean in dark blue and cyan curves.

the available reference measurements, we estimate the number of validated profiles to be too limited for a validation of our product.

A common approach to validate methane total column retrieval from shortwave infrared (SWIR) measurements is to compare the retrieved column to co-located ground-based measurements of the Total Carbon Column Observing Network (TCCON) (Wunch et al., 2011). Here, both the ground-based and satellite observations show homogeneous methane retrieval sensitivity over all atmospheric altitudes, leading to highly accurate estimates of the total column of methane rather than a profile. Because of the lack of other validation measurements, we decided to use these data for our product validation. In first instance, we derive a methane profile employing the MACC-II repository (Bergamaschi and Alexe, 2014), which delivers global methane fields on a daily basis, to extract an a priori estimate $\boldsymbol{x}_{\mathrm{apr}}$. This estimate is subsequently scaled to the total columns of co-located TCCON measurements. The profile is used to derive the total methane column as described by Eq. (11) and so the comparison

with TCCON total columns ensures the same null-space contribution in the GOSAT TIR and the validation estimate of the total column. Moreover, the MACC/TCCON profile can be used to compare to the methane profile $\boldsymbol{x}_\gamma$ in Eq. (7) and $\boldsymbol{x}_{\mathrm{CH_4}}$ in Eq. (10).

3.4 CH_4 retrievals

We start our validation analysis comparing the retrieved total methane columns from GOSAT-TIR measurements over TCCON stations with the corresponding measurements at the site. To minimise the interfering effect of scattering by clouds, hazes, cirrus, and/or aerosols, in this study we pertain tofocus on clear-sky conditions. This implies that a cloud-filter needs to be employed. Although, within the RemoTeC-framework, a well-tested cloud filter is available for daytime measurements over land based on SWIR and NIR spectra, there is no equivalent for the TIR spectrum. Particularly to filter nighttime measurements or measurements over the ocean, one has to resort to a cloud filter rooted in the TIR spectra. Therefore, we make use of the fact that clouds generally change the effective light path by scattering and the retrieved columns differ from the actual columns. For cloud clearingscreening of the data set, we consider the difference between the retrieved $\mathrm{N_2O}$ total column and the MACC $\mathrm{N_2O}$ total column. To account for an overall bias in the MACC $\mathrm{N_2O}$ columns, we define a dynamical mean x of the $\mathrm{N_2O}$ column errors such that cumulative number of converged retrievals in the range $[x-3\%, x+3\%]$ are maximised. All data within this interval are considered in the successive analysis to be cloud filtered. In Section 4.1 the cloud filter is investigated in more detail. Moreover, data are filtered using a stringent normed Pearson's chi-squared criterium of $\chi^2 < 3.0$ for the spectral fit quality. Figure 3 depicts the comparison between retrieved total methane columns from GOSAT-TIR measurements and co-located TCCON observations. Although, the GOSAT methane results capture the seasonal variation, they also clearly show a large and persistent bias of about 4.6%.

This bias shows little variation when compared to nine other TCCON sites (Bialystok, Bremen, Darwin, Lauder, Orleans, Park Falls, Reunion, Sodankyla, and Wollongong) as depicted in Figure 4. The error bars indicate the 1σ standard deviation of the difference between GOSAT and TCCON and correspond to a typical value of 2%. The propagation of the measurement noise into the retrieved total column amounts to retrieval error $\mathrm{s_{XCH_4}} \approx 0.8\%$ and explains only a part of spread. The average bias is $+4.6\%$, whereas the station-to-station variation in the bias is much smaller (0.4%). The accuracy of the total columns from the MACC repository, used as prior in the retrieval product, is also estimated to be of the order of 2%. This estimation is based on the study in Landgraf et al. (2016) where methane fields from the TM5 model are compared against GOSAT-SWIR retrievals and it was found that on average the standard deviations are well within 1%, with sporadic outliers up to 3%. It is noted that the TM5 model runs were conducted with methane constraints only taken from the measurements of the NOAA-ESRL global monitoring network, whereas within the MACC repository also the GOSAT-SWIR measurements are taken as input. In a study by Bergamaschi et al. (2009), the TM5 model with SCIAMACHY methane measurements as input, is verified. Also in this study, small deviations are found, typically in the order of 1%. This is even true for the stratosphere, where the model uncertainty is generally larger. Therefore, we believe that the estimation of 2% on the accuracy of the total columns from the MACC repository is reasonable, even on the safe side. Since it typically contributes for 30% to the retrieved total column, it contributes with $\approx 0.6\%$ to the error budget. Finally, the precision and accuracy of the methane TCCON measurements are

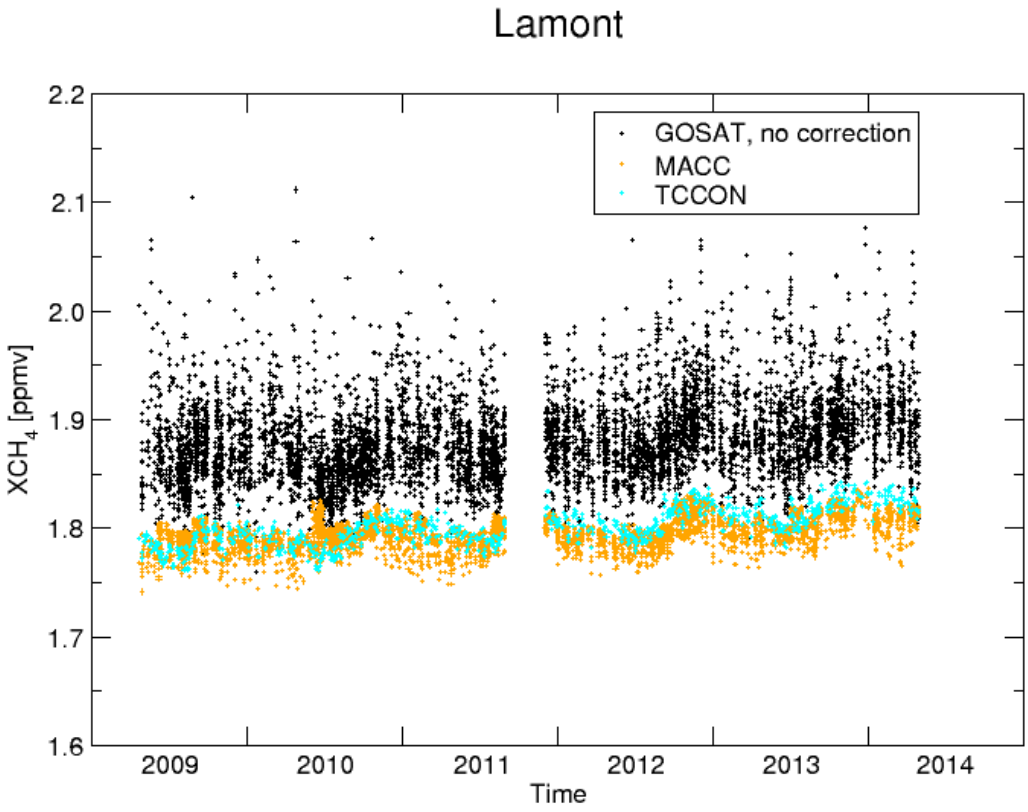

Figure 3. Total methane columns as a time series over Lamont. In black the GOSAT-TIR retrievals are shown. In respectively orange and cyan, the corresponding (non-scaled) MACC and TCCON total columns are shown.

both estimated to be $< 0.3\%$ (TCCON Data Description website). Overall these relatively small error contributions implies that further sources of uncertainties exist, e.g. radiometric calibration and forward model errors.

To better understand the induced errors, we compare the average GOSAT-TIR methane profile $\boldsymbol{x}_{\mathrm{CH_4}}$ over the TCCON site Bialystok with the averaged MACC/TCCON profile in Fig. 5. The deviation between the two profiles peaks around 9 km, which corresponds to the altitude of maximum retrieval sensitivity. This suggests that the altitude dependent bias in this figure finds its origin in the altitude dependent sensitivity. The depicted difference is indicatoryrepresentative for all TCCON stations.

Therefore, it is insightful to compare the retrieved GOSAT-TIR profiles $\boldsymbol{x}_\gamma$ in Eq. (4) with the smoothed MACC profile by applying the averaging kernel as indicated in Eq. (7). Figure 6 shows corresponding results for the TCCON site Bialystok. The bias on $\boldsymbol{x}_\gamma$ is much more constant over altitude, but still shows some striking vertical features with biases peaking around 9 km

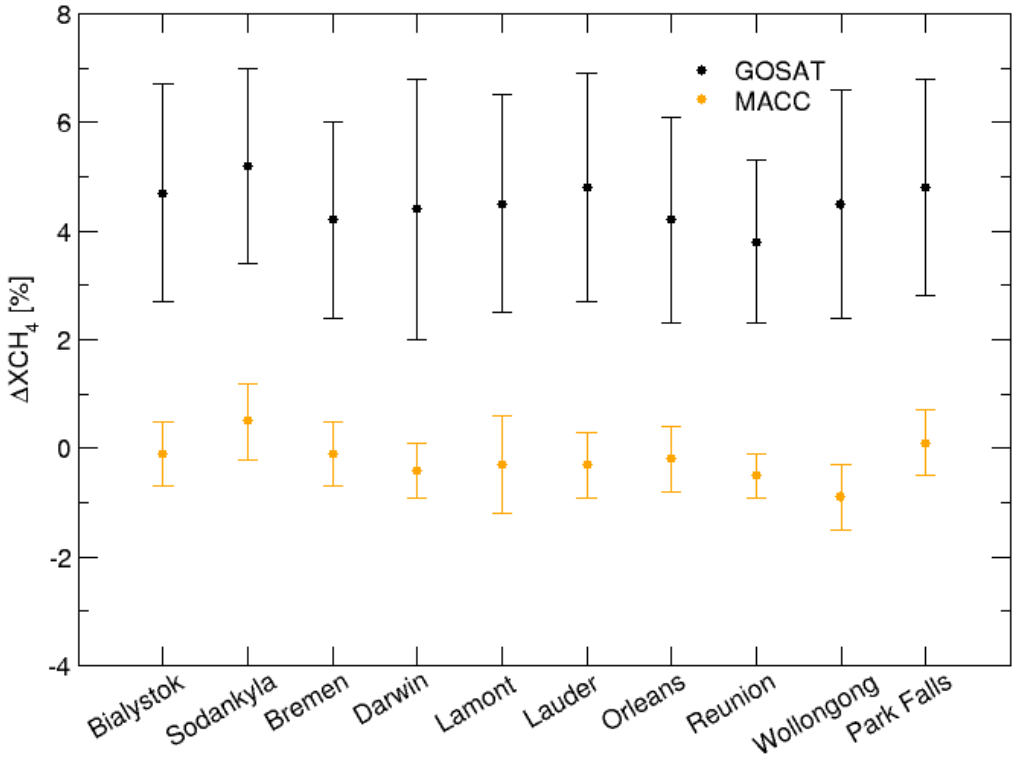

Figure 4. Average of the relative total methane column with respect to TCCON measurements for GOSAT-TIR retrievals (black) and the (non-scaled) MACC prior (orange). The bars indicate the spread in the data ensemble.

with the highest sensitivity to methane, a negative lobe towards lower altitudes and a sharp drop-off for the upper layers of the atmosphere.

To survey the retrieval performance at all TCCON sites mentioned in Table 1, Figure 7 shows the error bar chart of the mean retrieval bias at 2 and 9 km. Overall we see a similar behaviour for all TCCON sites and the station-to-station bias variation is small ($\approx 0.6\%$). Moreover, we find an interesting variation of biases for different types of observations, where we distinguish between daytime and nighttime observations and land and ocean scenes. In Fig. 7, the bias at 9 km is systematically lower for the daytime-land measurements than for the other three scenes, who are amongst themselves very comparable. At 2 km this behaviour is reversed; daytime-land measurements are systematically higher. For the interpretation, we have to consider the different retrieval sensitivity as indicated in Fig. 2. During day over land, the thermal contrast in the lower atmosphere is larger

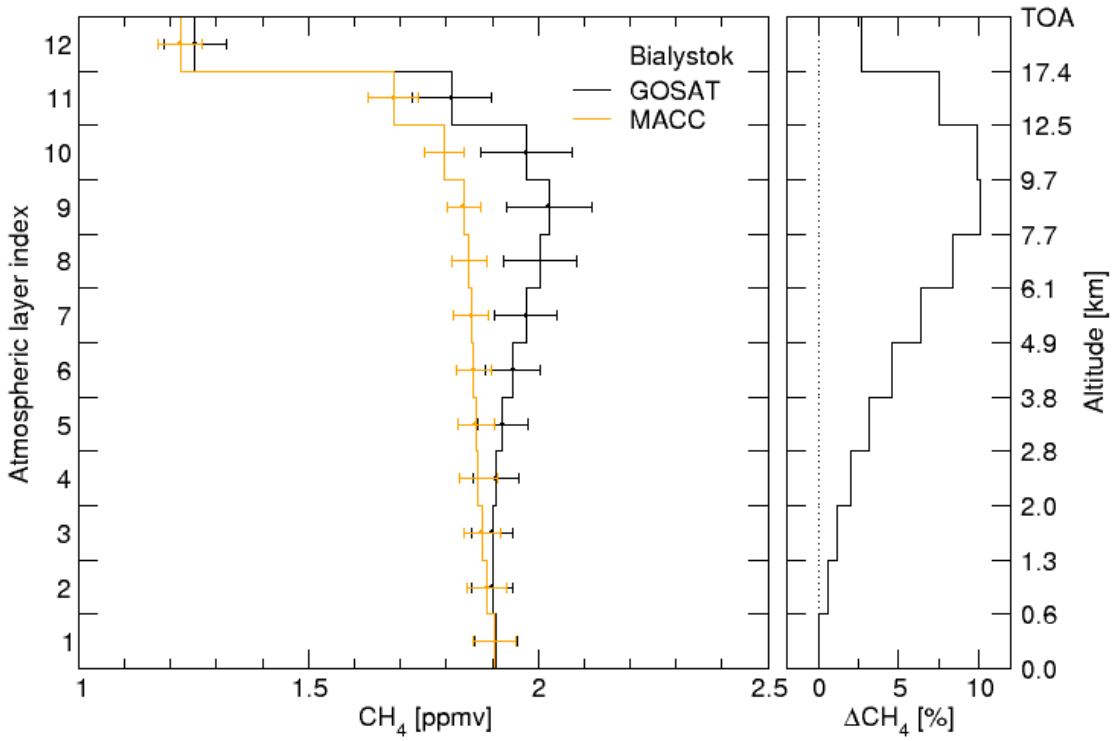

Figure 5. (left) Average methane profile retrieved from GOSAT-TIR spectra (black) over TCCON station Bialystok and from the MACC repository (orange) scaled such that the total column equals the corresponding TCCON total column measurement. The bars indicate the spread in the data ensemble. (right) The relative difference between the averaged retrieved GOSAT TIR and MACC methane profiles. It is noted that the two panels have different horizontal scales.

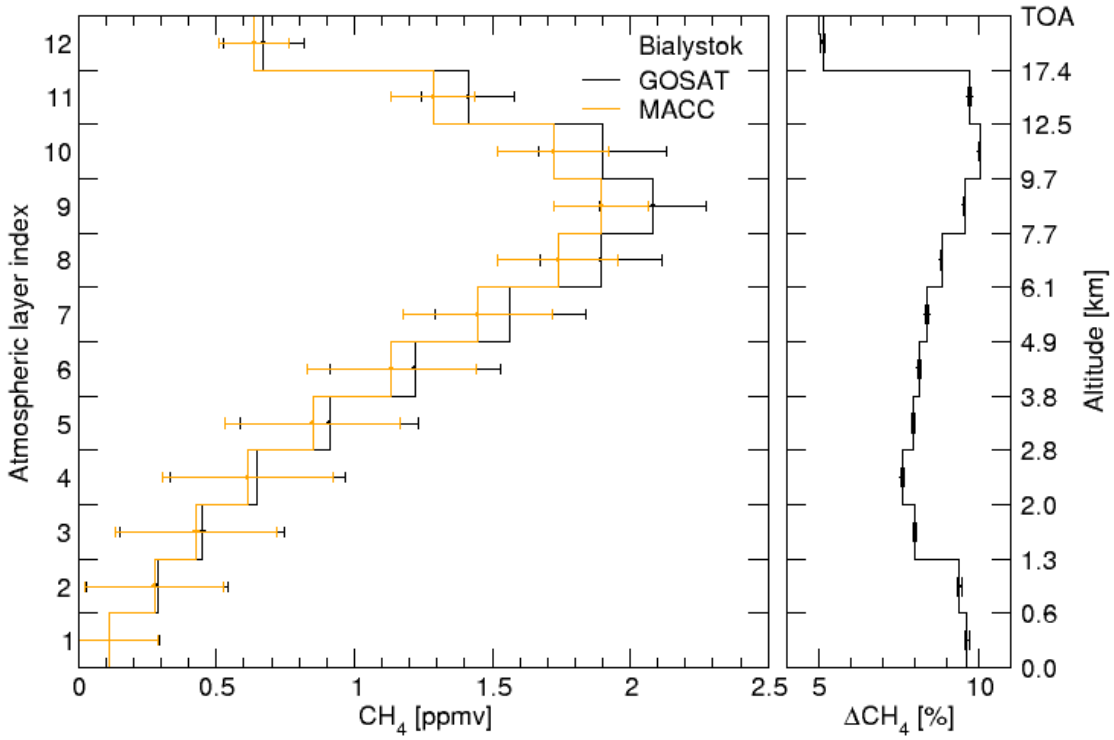

Figure 6. (left) Averaging kernel-smoothed profiles from GOSAT daytime measurements over land (black) and MACC (orange) at TCCON station Bialystok. The bars indicate the spread in the data ensemble. (right) The relative difference between the profiles. The bars pertain to the 1σ uncertainty of the averaged ratio, derived from the instrument noise propagation.

than for the other three cases and therefore the retrieval sensitivity increases accordingly. This enhancement goes along with larger biases.

Overall we conclude that the biases in the retrieved CH_4 profiles are significant and requires a mitigation strategy. A straightforward scaling of the retrieved profile by a certain factor is not sufficient because it cannot account for the altitude dependent biases for both $\boldsymbol{x}_\gamma$ and $\boldsymbol{x}_{CH_4}$. Therefore, in the next section we will discuss a scheme to correct radiometrically the GOSAT-TIR measurements as part of the inversion.

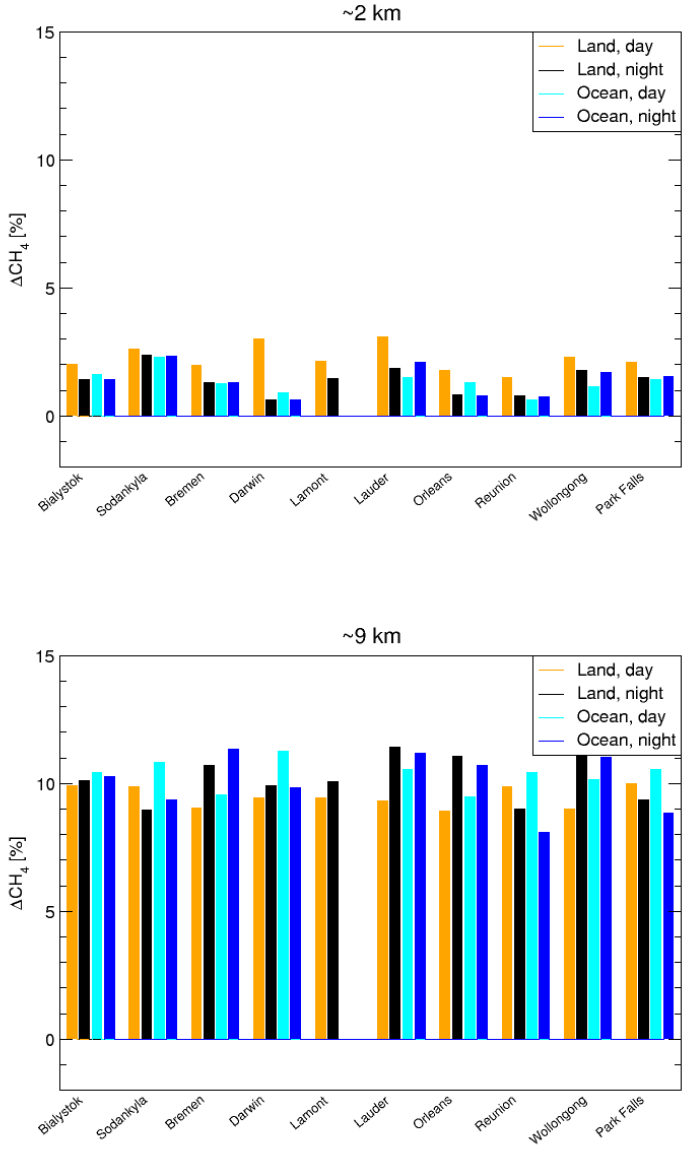

Figure 7. Histogram of the methane profile bias over ten different TCCON stations listed in Table 1, with the MACC/TCCON profiles as reference. The data are divided for different scenes; land and ocean scenes during daytime (respectively orange and cyan) and nighttime (respectively black and blue). In the left panel the deviation is shown for an altitude of ≈ 2 km and in the right panel of ≈ 9 km.

4 Bias correction scheme

Instead of correcting the biases at the level of geo-physical methane profiles, we consider an approach to quantify spectral features of radiometric biases of the GOSAT-TIR measurements. The observed methane bias finds its origin in the discrepancy $\boldsymbol{e_y}$ between forward model $\boldsymbol{F}$ and measurement $\boldsymbol{r}$ in Eq. (1). Although we cannot distinguish between forward model errors and instrumental errors, we can investigate the spectral properties of this discrepancy. Fixing the CH_4 and N_2O profile to accurate a priori knowledge, we retrieve all other parameters of the state vector, i.e. the skin temperature, a spectral shift, the total columns of H_2O and HDO, and an effectivea separate total H_2O column to calculate the water-continuum independently from the water vapour absorption lines. Analysing spectral fit residuals guides us to identify spectral components of the radiometric bias, that interfere with the atmospheric methane absorption. For this purpose we used CH_4 and N_2O data from the HIPPO (HIAPER Pole-to-Pole Observations) campaigns II and III (held in, respectively, October 2009 and March 2010). The HIPPO data contains vertical profiles of many relevant species and atmospheric parameters, setting strong constraints on the estimated state of the atmosphere. Although most of the measurements are taken over the Pacific ocean, in both campaigns vertical profiles have also been recorded over Northern America, and, in the case of campaign III, also over New Zealand. Therefore, these campaigns seem to suit our need to include as many as possible different scenes to investigate systematics in spectral residuals. With the co-location criteria ($\Delta\mathrm{lat} = 5°$, $\Delta\mathrm{lon} = 8°$, and $\Delta\mathrm{t} = 2$ hrs), the amount of unique HIPPO-GOSAT measurement pairs is ≈ 300.

Typically, the spectral residuals of this fit are very small, as can be seen in Figure 8. In the second panel, the noise level of a single measurement is indicated by the dashed line (7×10^{-8} W/m^2 sr cm^{-1}). The residual averaged over all co-located HIPPO-GOSAT pair is depicted in the third panel. Note that the spectral bias is less than 1% of the continuum level at 1210 cm^{-1}for the depicted spectrum, but causes biases in the retrieved methane product up to 10% at 9 km altitude.

The comparison of the second and third panel of Fig. 8 indicates that most residuals average out for larger data sets. This may be due to random noise contributions but also spectral features which change from observation to observation in a non-random manner are suppressed by the averaging. Here the principal component analysis (PCA) provides an adequate mean to detect non-random contributions in the fit residuals. It is based on an eigenvalue analysis of the covariance matrix of the underlying data set. The first principal component corresponds to the eigenvector with the largest possible variance, and for each succeeding component the variance degrades to lower values. By definition, the different principal components are uncorrelated.

Let $\mathbf{X}$ be the data matrix, consisting of 300 spectral residuals for all co-located HIPPO-GOSAT pairs, assuming that the mean residual is subtracted. Its covariance matrix $\mathbf{C}$ is then

$$\mathbf{C} = \mathbf{X}\mathbf{X}^{\mathrm{T}}/(n-1)\,, \tag{14}$$

which is symmetric and the eigenvalue problem can therefore be written as

$$\mathbf{C} = \mathbf{V}\mathbf{L}\mathbf{V}^{\mathrm{T}}, \tag{15}$$

with $\mathbf{L}$ a diagonal matrix with the eigenvalues of $\mathbf{C}$ and $\mathbf{V}$ the set of eigenvectors. When $\mathbf{L}$ contains the eigenvalues in decreasing order, then the i^{th} principal component is the i^{th} column of $\mathbf{V}$.

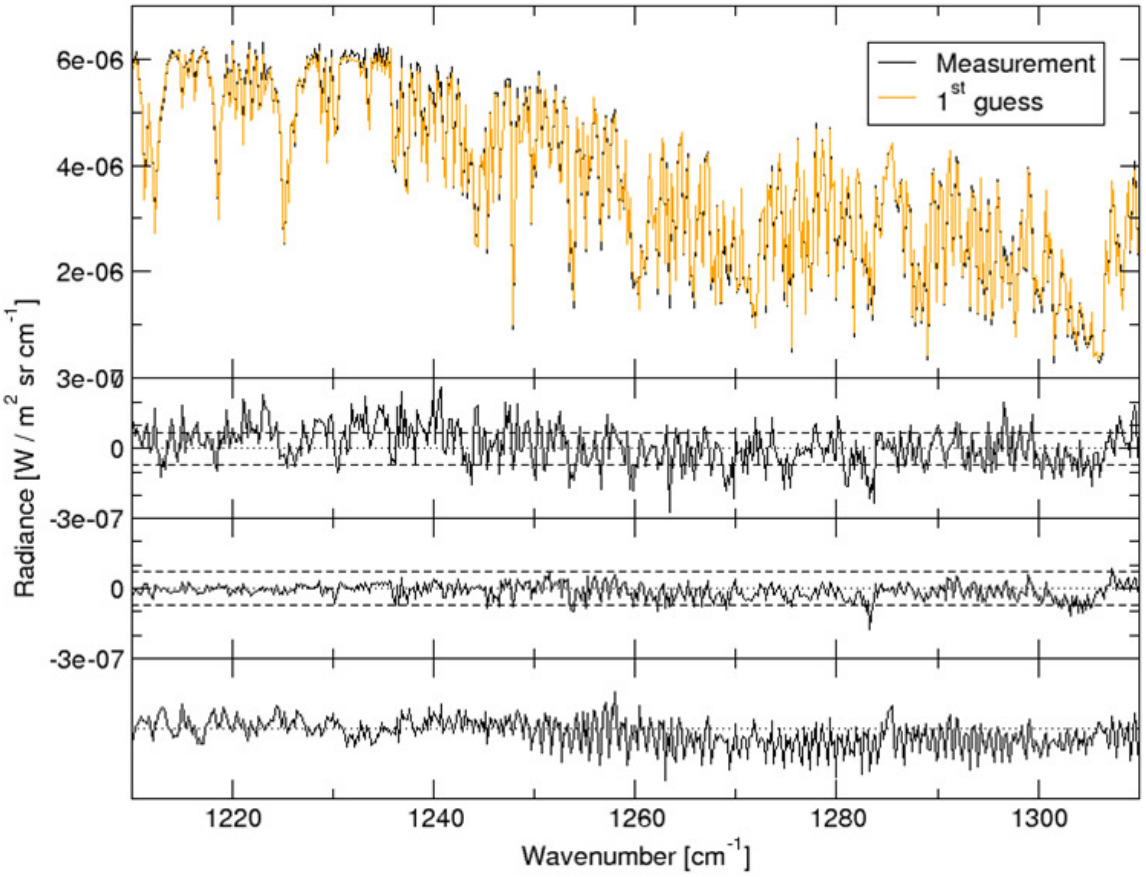

Figure 8. Comparison of GOSAT-TIR measurement with a forward model calculation based on methane profiles as measured during the HIPPO campaigns. The upper panel shows a single GOSAT measurement (black) and the forward calculation based on the co-located HIPPO measurement (orange), and in the second panel the residual is shown. The third panel depicts the average residual of all 300 GOSAT-HIPPO pairs used to centre all residuals in the principal component analysis. In the bottom panel the first principal component of this analysis is pictured.

25 The first principal component is shown in the fourth panel of Fig. 8. The strongest spectral features in this component show above 1250 $\mathrm{cm}^{-1}$and follow mostly $\mathrm{N_2O}$ and $\mathrm{CH_4}$ lines. In fact, this wavelength range corresponds to the part of the measurement where $\mathrm{N_2O}$ and $\mathrm{CH_4}$ are strongly interfering. Between 1210 $\mathrm{cm}^{-1}$and 1250 cm^{-1}some weak features coincide with water and methane lines. These coincidences may point to errors in the spectroscopy databases. However, they may also point to broadband radiometric biases, such as atmospheric continuum contributions or non-linear instrumental effects. The

impact of such effects on the spectrum is a function of the total optical density, explaining the different size of the spectral features in the component below and above 1250 cm^{-1}.

4.1 Bias-corrected methane retrievals

The first step of assessing the radiometric bias comprises the subtraction of the averaged residual from every GOSAT measurement before conducting a retrieval. In addition, we modify the forward model $\boldsymbol{F}$ by

$$\tilde{\boldsymbol{F}}(\boldsymbol{x}) = \boldsymbol{F}(\boldsymbol{x}) + \sum_i a_i \boldsymbol{p}_i \tag{16}$$

adding principal components $\boldsymbol{p}_i$ with the amplitudes a_i to be determined by the retrieval. Obviously, every addition of a principal component improves the spectral fit quality indicated by smaller χ^2 values, but on the other hand, it increases noise propagation and instability of the retrieval. Therefore, a trade-off needs to be made between bias-mitigation and reduced precision. Adding the first principal component to $\tilde{\boldsymbol{F}}$, improves the overall shape of the inferred methane profile, lowering the overall bias. The noise propagation, on the other hand, is only slightly increased with respect to the retrievals without this retrieved scaling parameter. Accounting for additional principal components leads hardly to any improvement in the bias but does increase the standard deviation in the differences between retrieved and reference methane profiles and is henceforward not considered in this study.

The effect of including this bias-correction scheme in the retrieval algorithm on the retrieved methane profile is depicted in Figure 9. On the left in this figure the profiles from bias-corrected GOSAT-TIR measurements are depicted for different scenes with the scaled MACC profile as a reference. It is noted that only the MACC profile for the daytime land case is depicted as the profiles for the other scenes are very similar and have been left out for clarity. On the right the averaged difference between GOSAT and MACC is depicted and it clearly the bias in the profiles is almost fully corrected for. The bias is within 2% over the whole altitude range. Also the spread in the ensemble, given by the error bars is lower than in the non-corrected case (from ≈ 0.10 ppmv to ≈ 0.08 ppmv at 9 km). In addition, the different retrieval performances for daytime and nighttime measurements, observations over land and ocean have been reduced and the daytime measurements over land are in line with the other three types of measurements.

For the other TCCON stations similar behaviour is found as can be seen in Fig. 10. For the retrieved methane concentration at 9 km altitude, the mean bias is -0.08% and the 1σ station-to-station variation in the bias is 0.76%. At this altitude, the discrepancy between daytime over-land scenes and the other three scenes is small (mean biases are respectively -0.31% and -0.01%; station-to-station variations are 0.83% and 0.72%). For 2 km altitude, we find that daytime over-land measurements show a systematic positive bias over all TCCON stations (mean bias is 0.97% with a station-to-station variation of 0.53%), whereas for the nighttime and ocean measurements, the corresponding biases are much smaller (mean of 0.07% and a variation of 0.16%). The daytime over-land biases may be explained by the fact that the HIPPO measurements are predominantly performed over the Pacific, and the few over-land measurements are not sufficiently different to fully account for the variability in the spectral residuals of all different scenes. Therefore, it may be that the correction is most applicable for scenes with a

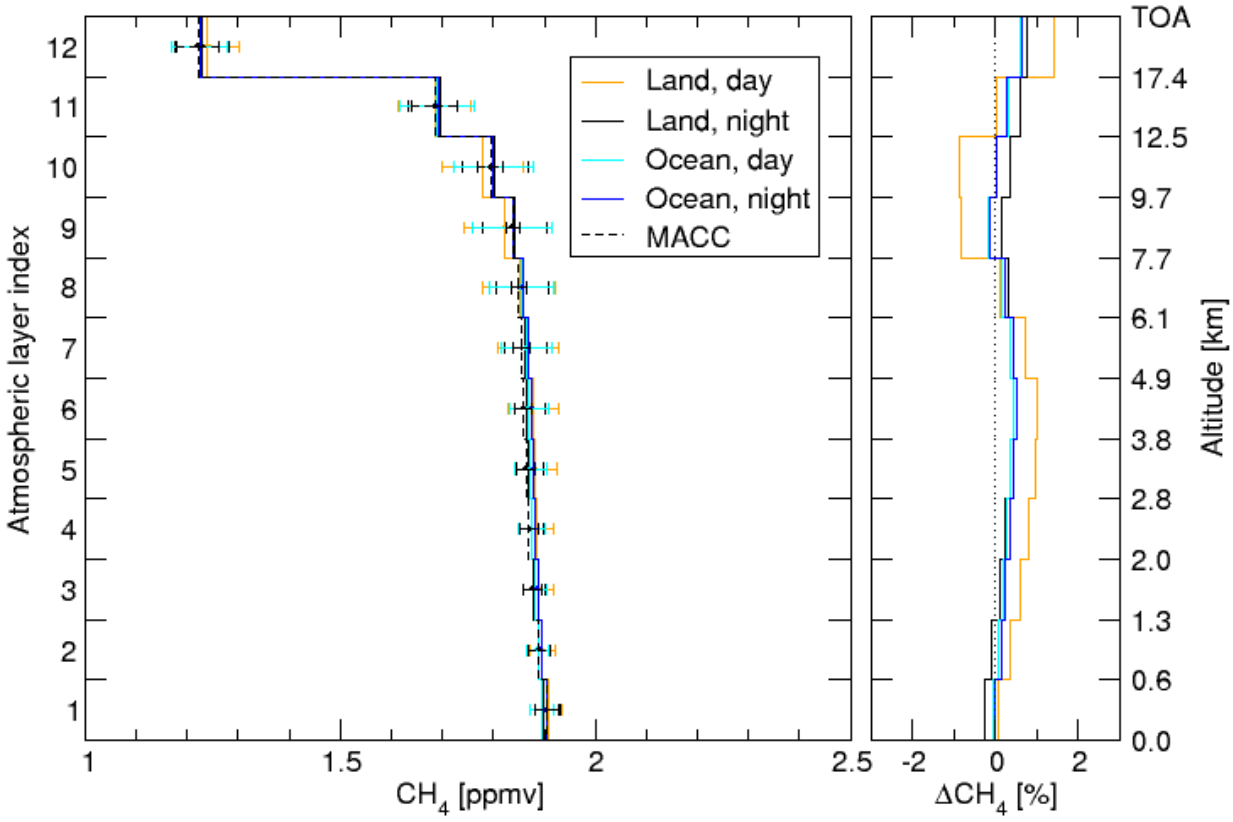

Figure 9. (left) Retrieved methane profiles from GOSAT-TIR measurements over TCCON station Bialystok with the bias-correction scheme included in the retrieval algorithm. The data are divided for different scenes; land and ocean scenes during daytime (respectively orange and cyan) and nighttime (respectively black and blue). The dashed lines refer to the MACC profiles for the daytime land scenes, and are very similar to the profiles for the other 3 scenes and have been left out for clarity. (right) The relative difference between the GOSAT-TIR retrievals and the MACC profiles.

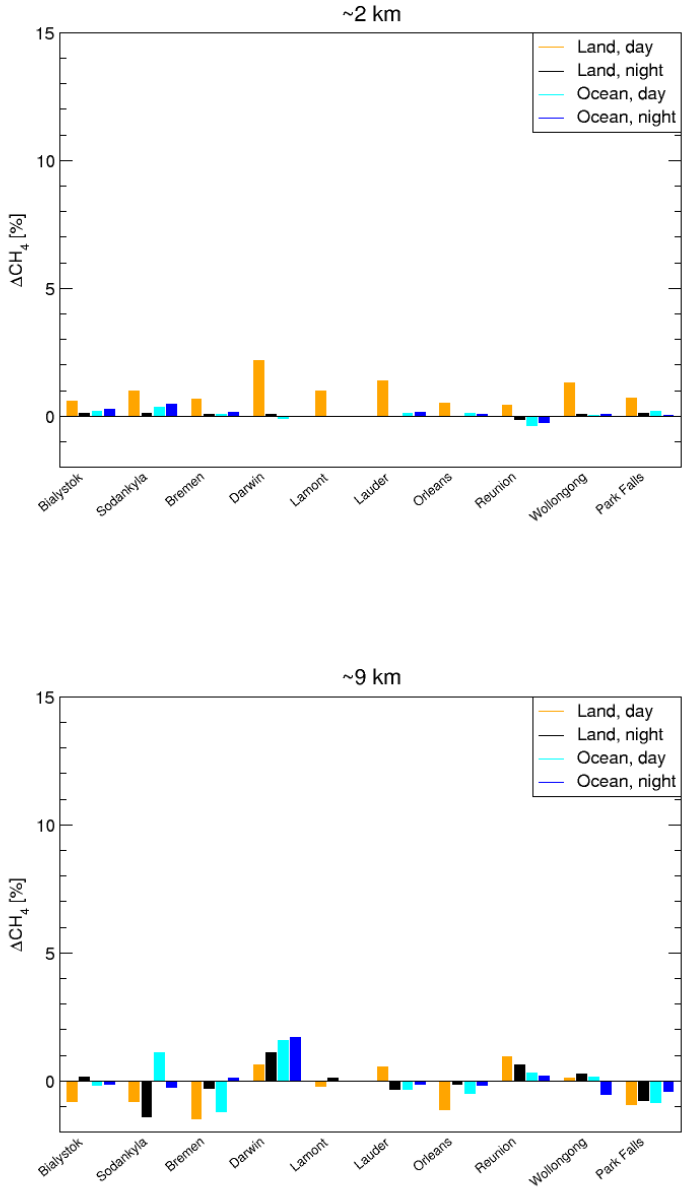

Figure 10. Bar-graphs for the relative deviation in the partial methane column at ≈ 2 km altitude (left) and ≈ 9 km (right) for ten different TCCON stations. The data are divided for different scenes; land and ocean scenes during daytime (respectively orange and cyan) and nighttime (respectively black and blue).

Table 1. Total methane column retrieval results after applying the bias-correction scheme for scenes over land during daytime. The first three columns pertain to the cloud filter based on fit parameters of GOSAT-TIR retrievals, whereas the last three columns refer to the filtering exploiting spectral features in GOSAT SWIR and NIR spectra. The average remaining bias is given for each TCCON station used in the current study along with the 1σ spread and the number of measurements passing the particular filter. The last two rows show the values for the whole ensemble.

Station	TIR filtered			SWIR filtered		
	b	σ	n	b	σ	n
Bialystok	0.4	2.2	3370	0.8	1.4	355
Sodankyla	0.7	1.7	486	0.9	0.8	9
Bremen	0.1	2.1	1366	0.2	1.2	212
Darwin	1.3	2.1	1542	0.5	1.1	463
Lamont	0.6	2.1	6985	0.4	1.2	2307
Lauder	1.3	3.1	187	0.4	1.8	27
Orleans	0.1	1.9	3023	0.4	1.1	384
Reunion	0.7	1.8	194	0.9	1.1	48
Wollongong	0.9	2.4	2121	0.6	1.3	407
Park Falls	0.3	2.2	4367	0.6	1.3	947
$\bar{b}$	0.6	2.2		0.6	1.2	
σ_b	0.4	-		0.2	-	

low thermal contrast. In the future, this shortcoming of our bias correction can be improved upon by an extended ensemble of airborne measurements, including over-land CH_4 and N_2O measurements.

After establishing the bias correction, we finally consider the efficiency of the TIR cloud filter as discussed in Sec. 3.4. For GOSAT daytime over-land measurements, we compare the efficiency of the TIR cloud filter with that of the RemoTeC cloud clearingscreening for the SWIR retrievals. Table 1 displays the average bias b and its standard deviation σ for GOSAT-TIR retrievals applying the two different cloud filters to the data. From the table it can be seen that the number of scenes n passing the TIR filter is significantly higher than for the SWIR filter. The average results are consistent with both filtering methods as the mean bias of all stations is $\bar{b} = +0.6\%$ for both cloud filters. However, the station-to-station scatter in the bias σ_b, defined as the standard deviation of the mean biases per station, is 0.4% and 0.2% for the TIR and SWIR cloud filtered data, respectively. Also the scatter in the data are significantly lower in case of the SWIR cloud filter (1.2%) compared to the TIR filter (2.2%). It is noted that constraining the TIR filter criteria more stringently does not lead to a reduced scatter.

For the daytime land retrievals one may therefore consider to apply the SWIR filtering. However, this is not possible for ocean and nighttime observations. For consistency reasons we only consider TIR cloud filtering for all observations in this study.

We conclude that the cloud filter using SWIR spectral features is more able to filter GOSAT observations with respect to cloudiness than the TIR data filtering. However, on average both cloud filters are consistent and the cloud filter using TIR data does not introduce additional biases in the methane product.

5 Conclusions

Methane profile retrievals generally result in a positive bias when retrieved from thermal infrared spectra. In case of GOSAT TIR, this bias is 4–5% in the total methane column, and can amount to 10% at altitudes where the sensitivity peaks (typically 9 km). To account for this bias, a correction scheme has been developed. It has been shown that a simple additive or multiplicative scheme may result in a sufficiently accurate total methane column product, but that such schemes are insufficient to account for nonphysical structures in the retrieved profiles. In fact, these structures only yield correct total columns when they properly cancel. Especially in cases with enhanced methane abundances, in particular close to the surface or at high altitudes, this presumption may not be valid. In view of inversion schemes to determine methane sources and sinks, it is these scenes with enhanced methane that are most interesting, but may lead to erroneous values. Moreover, land-ocean transitions and differences between day and night are also not fully corrected for with these simple correction schemes in the case of GOSAT-TIR data.

In this study, we have developed a more elaborate bias correction scheme to account for all these aspects in methane retrievals from GOSAT-TIR spectra. The scheme is rooted in a principal component analysis of the spectral residuals between measurement and a forward model run with the best possible knowledge of the state of the atmosphere. Pivotal in this knowledge are CH_4 and N_2O profiles which have been derived from HIPPO air campaign data. It has been shown that accounting for the average spectral residual and including one additional fitting parameter to scale the first principal component is sufficient to account for the bias within 2% when compared to the MACC methane fields (scaled to TCCON total columns). This is true for the whole altitude range from ground level to the top of the atmosphere and over all ten TCCON stations considered in this study. Moreover, the retrieval results from measurements over the ocean and the nighttime measurements over land, are all consistent with each other. Only at low altitudes, where the measurements have only limited sensitivity, the daytime measurements over land seem to show a persistent positive bias of $\approx 1\%$ at low altitudes. These scenes generally show a larger contrast between the Earth's skin temperature and the temperature of the lowest atmospheric levels, with respect to ocean scenes or nighttime observations. The reason that the bias correction scheme does not fully account for this bias in methane, may lie in the fact that the HIPPO campaigns are mostly performed over the Pacific, and the daytime land measurements may therefore be under-represented in the data set of residuals to be accounted for in a principal component analysis.

Nevertheless, the average bias in the retrieved GOSAT-TIR methane profile is less than 2% over the full altitude range, for all scenes over all TCCON stations, during day and night, when compared with MACC/TCCON values.

Acknowledgements.

References

Bergamaschi, P. and Alexe, M.: Report on the quality of the inverted CH4 fluxes (second report), Tech. Rep. MACC-II Deliverable D_43.4, Tech. Rep., Joint Research Center, European Commission, 2014.

Bergamaschi, P., Frankenberg, C., Meirink, J., Krol, M., Villani, M. G., Houweling, S., Dentener, F., Dlugokencky, E., Miller, J., Gatti, L., Engel, A., and Levin, I.: Inverse modeling of global and regional CH4 emissions using SCIAMACHY satellite retrievals, J. Geophys. Res., 114, D22 301, doi:10.1029/2009JD012287, 2009.

Borbas, E. and Ruston, B.: The RTTOV UWiremis IR land surface emissivity module, http://nwpsaf.eu/vs_reports/nwpsaf-mo-vs-042.pdf, 2010.

Borbas, E., Knuteson, R., Seemann, S., Weisz, E., Moy, L., and Huang, H.-L.: A high spectral resolution global land surface infrared emissivity database, in: Joint 2007 EUMETSAT Meteorological Satellite Conference and the 15th Satellite Meteorology & Oceanography Conference of the American Meteorological Society, Amsterdam, The Netherlands, http://www.eumetsat.int/home/Main/Publications/Conference_and_Workshop_Proceedings/groups/cps/documents/document/pdf_conf_p50_s10_03_borbas_p.pdf, 2007.

Borsdorff, T., Hasekamp, O. P., Wassmann, A., and Landgraf, J.: Insights into Tikhonov regularization: application to trace gas column retrieval and the efficient calculation of total column averaging kernels, Atmos. Meas. Tech., 7, 523–535, doi:10.5194/amt-7-523-2014, 2014.

Bousserez, N., Henze, D., Perkins, A., Bowman, K., Lee, M., Liu, J., Deng, F., and Jones, D.: Improved analysiserror covariance matrix for high-dimensional variational inversions: application to source estimation using a 3D atmospheric transport model, doi:doi:10.1002/qj.2495, 2015.

Brenninkmeijer, C., Crutzen, P., Boumard, F., Dauer, T., Dix, B., Ebinghaus, R., Filippi, D., Fischer, H., Franke, H., Frieß, U., Heintzenberg, J., Helleis, F., Hermann, M., Kock, H., Koeppel, C., Lelieveld, J., Leuenberger, M., Martinsson, B., Miemczyk, S., Moret, H., Nguyen, H., Nyfeler, P., Oram, D., O'Sullivan, D., Penkett, S., Platt, U., Pupek, M., Ramonet, M., Randa, B., Reichelt, M., Rhee, T., Rohwer, J., Rosenfeld, K., Scharffe, D., Schlager, H., Schumann, U., Slemr, F., Sprung, D., Stock, P., Thaler, R., Valentino, F., van Velthoven, P., Waibel, A., Wandel, A., Waschitschek, K., Wiedensohler, A., Xueref-Remy, I., Zahn, A., Zech, U., , and Ziereis, H.: Civil Aircraft for the regular investigation of the atmosphere based on an instrumented container: The new CARIBIC system, Atmos. Chem. Phys., 7, 4953–4976, doi:10.5194/acp-7-4953-2007, 2007.

Butz, A., Guerlet, S., Hasekamp, O., Schepers, D., Galli, A., Aben, I., Frankenberg, C., Hartmann, J.-M., Tran, H., Kuze, A., Keppel-Aleks, G., Toon, G., Wunch, D., Wennberg, P., Deutscher, N., Griffith, D., Macatangay, R., Messerschmidt, J., Notholt, J., , and Warneke, T.: Toward accurate CO2 and CH4 observations from GOSAT, Geophys. Res. Lett., 38, L14 812, doi:10.1029/2011GL047888, 2011.

CarbonTracker website: http://carbontracker.noaa.gov.

Cressot, C., Chevallier, F., Bousquet, P., Crevoisier, C., Dlugokencky, E., Fortems-Cheiney, A., Frankenberg, C., Parker, R., Pison, I., Scheepmaker, R., Montzka, S., Krummel, P., Steele, L., and Langenfelds, R.: On the consistency between global and regional methane emissions inferred from SCIAMACHY, TANSO-FTS, IASI and surface measurements, Atmos. Chem. Phys., 14, 577–592, doi:10.5194/acp-14-577-2014, 2014.

Crevoisier, C., Nobileau, D., Armante, R., Crépeau, L., Machida, T., Sawa, Y., Matsueda, H., Schuck, T., Thonat, T., Pernin, J., Scott, N., and Chédin, A.: The 2007-2011 evolution of tropical methane in the mid-troposphere as seen from space by MetOp-A/IASI, Atmos. Chem. Phys., 13, 4279–4289, doi:10.5194/acp-13-4279-2013, 2013.

Dee, D., Uppala, S., Simmons, A., Berrisford, P., Poli, P., Kobayashi, S., Andrae, U., Balmaseda, M., Balsamo, G., Bauer, P., Bechtold, P., Beljaars, A., van de Berg, L., Bidlot, J., Bormann, N., Delsol, C., Dragani, R., Fuentes, M., Geer, A., Haimberger, L., Healy, S., Hersbach, H., Hólm, E., Isaksen, L., Kållberg, P., M.Köhler, Matricardi, M., McNally, A., Monge-Sanz, B., Morcrette, J.-J., Park, B.-K., Peubey, C., de Rosnay, P., Tavolato, C., Thépaut, J.-N., and Vitart, F.: The ERA-Interim reanalysis: configuration and performance of the data assimilation system, Q. J. R. Meteorol. Soc., 137, 553–597, doi:10.1002/qj.828, 2011.

Hansen, P.: Analysis of discrete ill posed problems by means of the L-curve, SIAM Rev., 34, 561–580, 1992.

Holl, G., Walker, K., Conway, S., Saitoh, N., Boone, C., Strong, K., and Drummond, J.: Methane cross-validation between three Fourier transform spectrometers: SCISAT ACE-FTS, GOSAT TANSO-FTS, and ground-based FTS measurements in the Canadian high Arctic, Atmos. Meas. Tech., 9, 1961–1980, doi:10.5194/amt-9-1961-2016, 2016.

Inoue, M., Morino, I., Uchino, O., Miyamoto, Y., Saeki, T., Yoshida, Y., Yokota, T., Sweeney, C., Tans, P., Biraud, S., Machida, T., Pettman, J., Kort, E., Tanaka, T., Kawakami, S., Sawa, Y., Tsuboi, K., and Matsueda, H.: Validation of XCH4 derived from SWIR spectra of GOSAT TANSO-FTS with aircraft measurement data, Atmos. Meas. Tech., 7, 2987–3005, doi:10.5194/amt-7-2987-2014, 2014.

Jacob, D., Turner, A., Maasakkers, J., Sheng, J., Sun, K., Liu, X., Chance, K., Aben, I., McKeever, J., and Frankenberg, C.: Satellite observations of atmospheric methane and their value for quantifying methane emissions, Atmos. Chem. Phys., 16, 14 371–14 396, doi:10.5194/acp-16-14371-2016, 2016.

Karion, A., Sweeney, C., Tans, P., and Newberger, T.: AirCore: An Innovative Atmospheric Sampling System, J. Atmos. Ocean. Tech., 27, 1839–1853, doi:10.1175/2010JTECHA1448.1, 2010.

Kuze, A., Suto, H., Nakajima, M., and Hamazaki, T.: Thermal and near infrared sensor for carbon observation Fourier-transform spectrometer on the Greenhouse Gases Observing Satellite for greenhouse gases monitoring, Appl. Opt., 48, 6716–6733, doi:10.1364/AO.48.006716, 2009.

Kuze, A., Taylor, T., Kataoka, F., Bruegge, C., Crisp, D., Harada, M., Helmlinger, M., Inoue, M., Kawakami, S., Kikuchi, N., Mitomi, Y., Murooka, J., Naito, M., D.M. O'Brien, C. O., Ohyama, H., Pollock, H., Schwandner, F., Shiomi, K., Suto, H., Takeda, T., Tanaka, T., Urabe, T., Yokota, T., and Yoshida, Y.: Long term vicarious calibration of GOSAT sensors; techniques for error reduction and new estimates of degradation factors, I.E.E.E. Trans. Geosci. Remote Sens., 52, 3991–4004, doi:10.1109/TGRS.2013.2278696, 2014.

Kuze, A., Suto, H., Shiomi, K., Kawakami, S., Tanaka, M., Ueda, Y., Deguchi, A., Yoshida, J., Yamamoto, Y., Kataoka, F., Taylor, T., , and Buijs, H.: Update on GOSAT TANSO-FTS performance, operations, and data products after more than 6 years in space, Atmos. Meas. Tech., 9, 2445–2461, doi:10.5194/amt-9-2445-2016, 2016.

Landgraf, J., aan de Brugh, J., Scheepmaker, R., Borsdorff, T., Hu, H., Houweling, S., Butz, A., Aben, I., and Hasekamp, O.: Carbon monoxide total column retrievals from TROPOMI shortwave infrared measurements, Atmos. Meas. Tech., 9, 4955–4975, doi:10.5194/amt-9-4955-2016, 2016.

Machida, T., Matsueda, H., Sawa, Y., Nakagawa, Y., Hirotani, K., Kondo, N., Goto, K., Nakazawa, N., Ishikawa, K., and T.Ogawa: Worldwide measurements of atmospheric CO2 and other trace gas species using commercial airlines, J. Atmos. Ocean. Tech., 25, 1744–1754, doi:10.1175/2008JTECHA1082.1, 2008.

Mlawer, E. J., Payne, V. H., Moncet, J.-L., Delamere, J. S., Alvarado, M. J., and Tobin, D. C.: Development and recent evaluation of the MT_CKD model of continuum absorption, Phil. Trans. Roy. Soc. London Ser. A, 370, 2520–2556, doi:10.1098/rsta.2011.0295, 2012.

Myhre, G., Shindell, D., Bréon, F.-M., Collins, W., Fuglestvedt, J., Huang, J., Koch, D., Lamarque, J.-F., Lee, D., Mendoza, B., Nakajima, T., Robock, A., Stephens, G., Takemura, T., and Zhang, H.: Anthropogenic and Natural Radiative Forcing, in: Climate Change 2013: The Physical Science Basis. Contribution of Working Group I to the Fifth Assessment Report of the Intergovernmental Panel on Climate

Change, edited by Stocker, T., Qin, D., Plattner, G.-K., Tignor, M., Allen, S., Boschung, J., Nauels, A., Xia, Y., Bex, V., and Midgley, P., chap. 8, Cambridge University Press, Cambridge, United Kingdom and New York, NY, USA, 2013.

OCO-2: Orbiting Carbon Observatory-2 (OCO-2) Level 2 Full Physics Retrieval Algorithm Theoretical Basis, https://docserver.gesdisc.eosdis.nasa.gov/public/project/OCO/OCO2_L2_ATBD.V6.pdf.

O.P. Hasekamp, J. L.: Ozone profile retrieval from backscattered ultraviolet radiances: The inverse problem solved by regularization, J. Geophys. Rev., 106, 8077–8088, doi:10.1029/2000JD900692, 2001.

Peters, W., Jacobson, A., Sweeney, C., Andrews, A., an, T. C., Masarie, K., Miller, J., Bruhwiler, L. P., Petron, G., Hirsch, A., Worthy, D. J., van der Werf, G., Randerson, J., Wennberg, P., Krol, M., and Tans., P.: An atmospheric perspective on North American carbon dioxide exchange: CarbonTracker, Proc. Nat. Acad. Sc. USA, 104, 18 925–18 930, doi:10.1073/pnas.0708986104, 2007.

Phillips, P.: A technique for the numerical solution of certain integral equations of the first kind, J. Assoc. Comput. Mach., 9, 84–97, 1962.

Razavi, A., Clerbaux, C., Wespes, C., Clarisse, L., Hurtmans, D., Payan, S., Camy-Peyret, C., and Coheur, P.: Characterization of methane retrievals from the IASI space-borne sounder, Atmos. Chem. Phys., 9, 7889–7899, 2009.

Rothman, L., Gordon, I., Barbe, A., Benner, D. C., Bernath, P., Birk, M., Boudon, V., Brown, L., Campargue, A., Champion, J.-P., Chance, K., Coudert, L., Dana, V., Devi, V., Fally, S., Flaud, J.-M., Gamache, R., Goldman, A., Jacquemart, D., Kleiner, I., Lacome, N., Lafferty, W., Mandin, J.-Y., Massie, S., Mikhailenko, S., Miller, C., Moazzen-Ahmadi, N., Naumenko, O., Nikitin, A., Orphal, J., Perevalov, V., Perrin, A., Predoi-Cross, A., Rinsland, C., Rotger, M., Šimečková, M., Smith, M., Sung, K., Tashkun, S., Tennyson, J., Toth, R., Vandaele, A., and Auwera, J. V.: The HITRAN 2008 molecular spectroscopic database, J. Quant. Spectrosc. Radiat. Transfer, 110, 533–572, doi:10.1016/j.jqsrt.2009.02.013, 2009.

Saitoh, N., Imasu, R., Ota, Y., and Niwa, Y.: CO2 retrieval algorithm for the thermal infrared spectra of the Greenhouse Gases Observing Satellite: Potential of retrieving CO2 vertical profile from high-resolution FTS sensor, J. Geophys. Res., 114, D17 305, doi:10.1029/2008JD011500, 2009.

Saitoh, N., Touno, M., Hayashida, S., Imasu, R., Shiomi, K., Yokota, T., Yoshida, Y., Machida, T., Matsueda, H., and Sawa, Y.: Comparisons between XCH4 from GOSAT Shortwave and Thermal Infrared Spectra and Aircraft CH4 Measurements over Guam, SOLA, 8, 145–149, doi:10.2151/sola.2012-036, 2012.

Schepers, D., Guerlet, S., Butz, A., Landgraf, J., Frankenberg, C., Hasekamp, O., Blavier, J.-F., Deutscher, N., Griffith, D., Hase, F., Kyro, E., Morino, I., Sherlock, V., Sussmann, R., and Aben, I.: Methane retrievals from Greenhouse Gases Observing Satellite (GOSAT) shortwave infrared measurements: Performance comparison of proxy and physics retrieval algorithms, J. Geophys. Res., 117, D10 307, doi:10.1029/2012JD017549, 2012, 2012.

Seemann, S., Borbas, E., Knuteson, R., Stephenson, G., and Huang, H.-L.: Development of a Global Infrared Land Surface Emissivity Database for Application to Clear Sky Sounding Retrievals from Multi-spectral Satellite Radiance Measurements, J. Appl. Meteor. Climatol., 47, 108–123, doi:10.1175/2007JAMC1590.1, 2008.

Siddans, R., Knappett, D., Waterfall, A., Hurley, J., Latter, B., Kerridge, B., Boesch, H., and Parker, R.: Global height-resolved methane retrievals from the Infrared Atmospheric Sounding Interferometer (IASI) on MetOp, Atmos. Meas. Tech. Disc., 2016, 1–46, doi:10.5194/amt-2016-290, 2016.

Steck, T.: Methods for determining regularization for atmospheric retrieval problems, Appl. Opt., 41, 1788–1797, 2002.

TCCON Data Description website: https://tccon-wiki.caltech.edu/Network_Policy/Data_Use_Policy/Data_Description.

Tikhonov, A.: On the solution of incorrectly stated problems and a method of regularization, Dokl. Akad. Nauk SSSR, 151, 501–504, 1963.

Twomey, S.: On the numerical solution of Fredholm integral equations of the first kind by inversion of the linear system produced by quadrature, J. Assoc. Comput. Mach., 10, 97–101, 1963.

van Delst, P. and Wu, X.: A high resolution infrared sea surface emissivity database for satellite applications, in: Technical Proceedings of The Eleventh International ATOVS Study Conference, pp. 407–411, 2000.

von Clarmann, T., Höpfner, M., Kellmann, S., Linden, A., Chauhan, S., Funke, B., Grabowski, U., Glatthor, N., Kiefer, M., Schieferdecker, T., Stiller, G., and Versick, S.: Retrieval of temperature, H2O, O3, HNO3, CH4, N2O, ClONO2 and ClO from MIPAS reduced resolution nominal mode limb emission measurements, Atmos. Meas. Tech., 2, 159–175, 2009.

Wassmann, A., Landgraf, J., and Aben, I.: Ozone profiles from clear sky thermal infrared measurements of the Infrared Atmospheric Sounding Interferometer: A retrieval approach accounting for thin cirrus, J. Geophys. Res., 116, D22 302, doi:10.1029/2011JD016066, 2011.

Wecht, K., Jacob, D., Wofsy, S., Kort, E., Worden, J., Kulawik, S., Henze, D., Kopacz, M., and Payne, V.: Validation of TES methane with HIPPO aircraft observations: implications for inverse modeling of methane sources, Atmos. Chem. Phys., 12, 1823–1832, doi:10.5194/acp-12-1823-2012, 2012.

Worden, J., Kulawik, S., Frankenberg, C., Payne, V., Bowman, K., Cady-Peirara, K., Wecht, K., Lee, J.-E., and Noone, D.: Profiles of CH4, HDO, H2O, and N2O with improved lower tropospheric vertical resolution from Aura TES radiances, Atmos. Meas. Tech., 5, 397–411, doi:10.5194/amt-5-397-2012, 2012.

Worden, J., Turner, A., Bloom, A., Kulawik, S., Liu, J., Lee, M., Weidner, R., Bowman, K., Frankenberg, C., Parker, R., and Payne, V.: Quantifying lower tropospheric methane concentrations using GOSAT near-IR and TES thermal IR measurements, Atmos. Meas. Tech., 8, 3433–3445, 2015.

Wu, X. and Smith, W.: Emissivity of rough sea surface for 8-13 μm: modeling and verification, Appl. Opt., 36, 2609–2619, 1997.

Wunch, D., Toon, G., Blavier, J.-F., Washenfelder, R., Notholt, J., Connor, B., Griffith, D., Sherlock, V., and Wennberg, P.: The Total Carbon Column Observing Network, Phil. Trans. R. Soc. A, 369, 2087–2112, doi:10.1098/rsta.2010.0240, 2011.

Xiong, X., Barnet, C., Maddy, E., Sweeney, C., Liu, X., Zhou, L., and Goldberg, M.: Characterization and validation of methane products from the Atmospheric Infrared Sounder (AIRS), J. Geophys. Res., 113, 2005–2012, 2008.

Zou, M., Xiong, X., Saitoh, N., Warner, J., Zhang, Y., Chen, L., Weng, F., M., and Fan: Satellite observation of atmospheric methane: intercomparison between AIRS and GOSAT TANSO-FTS retrievals, Atmos. Meas. Tech., 9, 3567–3576, doi:10.5194/amt-9-3567-2016, 2016.